A Statistical Separation Standard and Risk-Throughput Modeling of the Aircraft Landing Process

A dissertation submitted in partial fulfillment of the requirements for the degree of Doctor of Philosophy at George Mason University

By

Babak Ghalebsaz Jeddi
Masters of Science
University of Cincinnati, 2004
Masters of Science
University of Tehran, 1997
Bachelor of Science
Sharif University of Technology, 1994

Director: John F. Shortle, Associate Professor
Department of Systems Engineering and Operations Research

Summer Semester 2008
George Mason University
Fairfax, VA

DEDICATION

I would like to dedicate my dissertation to independent thinkers, whose thoughts, research and words has been bringing wisdom to peace and human well-being. I shall dedicate the dissertation to those who have ever encouraged, invigorated or tried to improve Human Rights at GMU. The last, but not the least, I shall dedicate my dissertation to honesty, peace and freedom of speech without which no healthy and objective research can be maintained.

ACKNOWLEDGEMENT

No research can be accomplished without support of those connected with the researcher. I would like to express my gratitude to my family who I have always benefited from their support throughout my education. I shall acknowledge and appreciate the advice and support of my Ph.D. advisor, Dr. John Shortle throughout my Ph.D. studies at GMU. I shall extend my gratitude to the GMU faculty, especially my Ph.D. committee members, Drs George Donohue, Lance Sherry, and Edward Wegman, and chair of the SEOR Department Dr. Ariela Sofer. I would like to express my thanks to Wayne Bryant and Ed Johnson at NASA for supporting our research. Some GMU staff has been very helpful to my work and I hereby appreciate their help, despite my condemnation of GMU administrative system. I also should appreciate the support of my friends and colleagues in and outside GMU.

TABLE OF CONTENTS

LIST OF TABLES

LIST OF FIGURES

LIST OF ABBRIVIATIONS

CDF cumulative distribution function
DTW Detroit metropolitan Wayne county airport
FAA Federal Aviation Administration
FAF final approach fix
GA go-around
IAD inter arrival distance
IAF initial approach fix
IAP instrument approach procedure
IAT inter arrival time to FAF
IFR instrument flight rule
IMC instrument meteorological condition
LTI landing time interval to the runway threshold
MAP missed approach point
PDF probability distribution function
ROT runway occupancy time
SRO simultaneous runway occupancy
TRACON terminal radar approach control
WV wake vortex
nmi nautical mile
s second

ABSTRACT

A STATISTICAL SEPARATION STANDARD AND RISK-THROUGHPUT MODELING OF THE AIRCRAFT LANDING PROCESS

Babak Ghalebsaz Jeddi, Ph.D.

George Mason University, 2008

Dissertation Director: Dr. John F. Shortle

In the context of a high demand for runways as important scarce resources of the national air transportation system, this dissertation is concerned with the problem of determining the best separation between aircraft to maximize the *output* of the *landing system*. The risks of *wake vortex hazard* on the following aircraft and *simultaneous runway occupancy* shall be controlled. The following specific questions are addressed:

1. What are the stochastic characteristics of the aircraft landing process?
2. What parameters should a separation standard include?
3. How should the optimal levels of separation standard parameters be decided to maximize the system output?

The first question is answered by statistical analysis of aircraft landing track data using "multilateration surveillance system" at Detroit airport (DTW). We present probability distribution functions of Landing Time Intervals to the runway threshold, and aircraft Runway Occupancy Time, among other distributions. We suggest that the current

"minimum separation" standards for a given type of follow lead aircraft, e.g. a large aircraft following another large aircraft, (under Instrument Flight Rule) should be replaced by statistical separation standards (SSS). Our proposed standard, for a given type of follow-lead pair, specifies a target separation value, a lower specification limit, and a standard for the variance of the process.

The optimal level of target separation, which defines the optimal level of the system output, depends on the cost of avoiding the risks and the benefits gained from closer and more frequent landings. An operational procedure will be proposed to avoid the wake vortex hazard. We present optimization models to maximize the system output given cost and benefit factors. The models also provide a framework to estimate runway landing capacity (defined as average sustainable risk-free/safe landing) taking into account the uncertainty of the landing process. The capacity estimation is critical for planning and scheduling purposes. Estimated effects/benefits of reducing variance, of Landing Time Interval, on landing capacity are presented.

CHAPTER 1 INTRODUCTION

Demand for air transportation has been increasing. This results in an increase in demand for runways. Runways are also very expensive to build. As a result, runways are scarce and economically valuable resources of the air transportation network. This limitation and high demand may lead to safety concerns since the system tends to over utilize the runways in effort to squeeze the maximum utilization out of the scarce resource. This objective of this research is to determine how the system should operate in order to maximize productivity, *but also to maintain safety*. This dissertation specifically deals with the process of landing aircraft on a single runway.

This chapter first demonstrates the growth of demand for air transportation in quantitative terms following with a discussion on runway scarcity and landing safety. Some shortcomings of the current landing separation standards are explained. Then the questions addressed in this research are presented. Methodologies to solve and answer these questions are briefly discussed in this section.

1.1 Growth of Demand for Air Transportation

Demand for air transportation has been increasing and will continue to rise. Commercial air transportation is a fast growing industry in the world and in the United States. It is

also the dominant mode of international movements of passengers. Rodrigue *et al*. (2005) discuss the growth of demand for air transportation. They explain that both passenger and cargo traffic have grown rapidly in the past few decades. Both types of passenger and freight traffic have outpaced the growth of the broader global economy. By 2003, approximately 900,000 people were airborne on scheduled flights somewhere in the world at any one time; and worldwide, 1.6 billion passengers traveled by air transport in the centenary of the Wright Brothers' first flight. Alone, North America and Europe accounted for 70.4% of all passenger movements in 2000.

Air transportation's share of world trade in goods is more than 40% by value (Kasarda, Green, and Sullivan, 2004). In the United States, air transportation had grown at a rapid rate until 2001. The passenger miles have increased four times as fast as GDP growth, as shown in Figure 1.1 (Donohue 2004). Some forecasting models and predictions for air transport are also given in Ashford & Wright (1992).

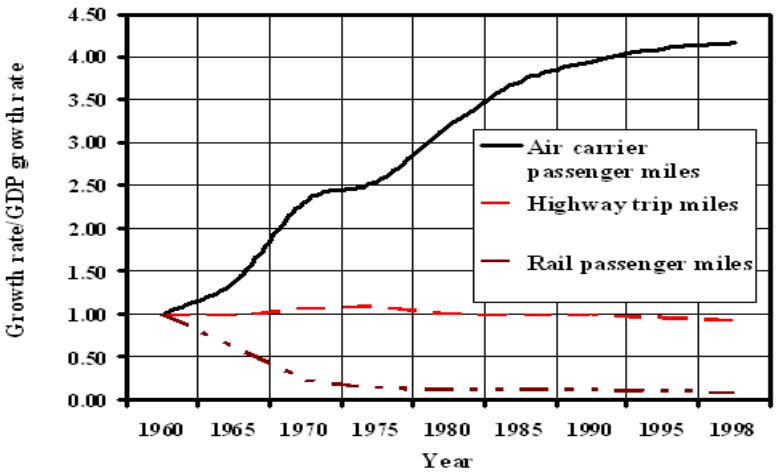

Figure 1.1. Passenger Miles vs. GDP

Before September 11, 2001, the FAA forecasted continued growth for commercial aviation as well as for general aviation during the first 10 years of the 21st century. The number of airplanes in operation will increase, and these airplanes will carry more people, fly more miles, and demand more resources both in airspace and airports. The FAA estimates that flight hours of commercial aviation will grow to 24 million hours in 2007 from 18 million in 1999, comparing with 8 million in 1982. The FAA projects that the use of large air carriers will grow at an annual rate of 4 percent, while the use of commuter air carriers will grow at 3 percent per year (GAO 2000). After the two-year recession due to September 11, 2001 event and economic stagnancy since year 2001, the industry is picking up the volume and growth rate. The latest forecast from FAA states that for the period 2005 to 2014 domestic passenger emplacements are expected to expand at an average annual rate of 3.8 percent in the next ten years, under the assumption that the U.S. economy grows at a moderate rate of 3.1 percent annually (FAA APO 2003).

As a result of growing air traffic demand, more operation volume both at en-route and airports is expected in the near future. [Extrapolation of] the historical data show that on average 14 more airplanes per month will be in operation with 1,000 million more passenger miles [by year 2020]. The 31 large hub airports in the US enplaned 439 million passengers in 2002. These airports are projected to enplane 793 million passengers in 2020, an 80.7 percent increase over the 18-year period (Xie 2005).

1.2 Runways as Scarce and Valuable Resources

All air transports start and end at runways, which implies increasingly high demand for runway slots (landing or departure) during peak periods at congested airports as demand for air transportation increases. Physical expansion of airport facilities (including runways) is one possible solution to the system congestion. However, the expansion is seriously confronted by limited geographical space, zoning and noise restrictions as well as the expense of building new runways. Also, the continuous residential and commercial growth around many airports does not allow space for more runways. An extension of operating hours to accommodate more traffic will also be challenged by the restrictions imposed for protection of communities surrounding the airports.

These factors along with the high demand have made runways very limiting and economically valuable resources of the air transportation network. To increase passenger throughput (and possibly reduce delays) it is desirable to obtain the maximum output of the runway operations whenever possible. In other words, a response to the resource scarcity is enhancing the runway utilization and throughput before investing on new runways.

Runway utilization or throughput is a function of the aircraft separation spacing on the glide path leading to the runway. However, *risk*, as the probability of loss of safety, is the other side of the *throughput* coin. Runway throughput can be increased by reducing in-trail landing separation between aircraft, but the consequence may be an increase in

the chance of a severe wake vortex encounter or a simultaneous runway occupancy or a costly go-around.

In this research, two major safety risks in aircraft landing procedures are considered. These are the risks of a wake vortex (WV) encounter and the risk of simultaneous runway occupancy (SRO). Other factors such as the presence of other kinds of vehicles on the runway are not included. A wake-vortex encounter occurs when the following aircraft enters the wake vortex of its leading aircraft. When the wake is strong enough, the encounter may cause a loss of control, which may result in passenger injuries or even fatalities. SRO risk is the probability that the following aircraft reaches the runway threshold before the leading aircraft exits the runway. A SRO is a precursor for a physical collision on the runway. These risks are to be avoided to assure a safe landing. Separation requirements which are designed to mitigate or eliminate these risks are the major constraints of the runway capacity. These separations shall be adjusted in the optimal level to assure a balanced trade-off between throughput, risk, and the cost of a go-around due to an unsuccessful landing.

1.3 Separation Standards

Current separation standards provide minima for any given follow-lead aircraft type as demonstrated in Table 1.1 for IFR (instrument flight rule) (FAA 1993). For example, under IFR, when a large aircraft is following a large aircraft, their distance to each other shall not be less than 3 nm when the leading aircraft is over the runway threshold. In some special cases 3 nm is allowed to be reduced to 2.5 nm. These minima were designed

in the 1970's to avoid the two aforementioned landing risks. Under IFR, the air traffic controller (ATC) is responsible to guide aircraft/pilots to assure the separation minima. It is assumed that if these minima are strictly respected, no aircraft crosses the threshold to land while the lead aircraft is still on the runway. These minima are supposed to be fully respected and are not to be violated. However, in practice they are frequently violated, as will be shown in this dissertation. Several empirical studies (e.g., Levy 2003) have analyzed statistics of the landing process and support this fact. For example, based on the observations in Jeddi *et al*. (2006) about 8% and 26% of landings (under IFR and 3 nm pairs of Table 1.1) have an inter-arrival distance under 2.5 nm and 3 nm, respectively (see Levy 2003 and Ballin 1996 for other examples).

Table 1.1. IFR approach in-trail, threshold separation minima (nmi)

FOLLOW AIRCRAFT	LEAD AIRCRAFT			
	SMALL	LARGE	B757	HEAVY
SMALL	3	4	5	6
LARGE	3	3	4	5
B757	3	3	4	5
HEAVY	3	3	4	4

These high percentages hint to two weaknesses of the current standards. First, if they are not to be violated, then the frequency of violation should not as high as has been observed. This can be seen as a pragmatic incompetence of these standards. Second, despite the high percentage of incidents in which aircraft are closer than the minima,

there are not so many wake vortex related incidents. One reason can be that wake vortex encounters are not always reported. Although this might be true, it does not question the fact because there has been no serious WV incident where these data are observed. Thus these standards may be overly conservative. This leads to under-utilization and loss of valuable runway capacity.

On the other hand, separation minima as standards are not directly operational. Because distance adjustment involves uncertainties so air traffic controllers (and pilots) add some buffer spacing to a given minimum and adjust the separation around a buffered distance to secure the required minimum. This issue is suggested and studied by some researchers, for example, Lebron (1987), Vandevinne *et al*. (1992), Sherry *et al*. (1999), and Jeddi *et al*. (2006b)[1]. In other words, by providing separation minima only, the current separation standards do not directly incorporate uncertainty of the process. We will show that the nature of current standards (as minima) systemically increases the separation variance which is undesirable (Jeddi *et al*. 2006).

An effective separation design shall address two challenges. First it shall control the risk of a severe wake vortex encounter and a simultaneous runway occupancy (or go-around) under peak operations. Secondly it should possibly reduce inherent variability of the separation spacing, which may result in increasing the throughput without increasing the risk. One of the hypotheses in this study is that the current separation design or standards does not posses these characteristics besides other aforementioned limitations.

[1] The paper is presented in chapter 4 of the dissertation.

Proposing a framework to set different types of separation standards to compensate for the weaknesses of the current standards is one purpose of this research, among other research questions which are described in the next section.

1.4 Research Questions

In the context of high demand for runways and their scarcity, this research is concerned with the problem of how the landing system (in terms of the separation planning and control) should operate so that it is safe and productive at the same time.

The problem is to decide the best separation between a given type of follow-lead aircraft to maximize the system output considering the risks of wake vortex hazard and simultaneous runway occupancy. Furthermore, there is a need to design a statistical mechanism to monitor and control the decided separation. The goal is to increase the system productivity which will benefit the stakeholders including passengers, airlines, airports, employees, and the economy in general. Through this research, performance metrics of the (landing) system are throughput, risk, and economic level of operations. The following questions will be addressed in this dissertation:

1. What are the probabilistic characteristics of the variables in the landing process, and what is the current level of risk (or safety) and throughput?
2. What parameters should a separation standard include to function as an operational guideline and to directly account for variability in the process?

3. How should the optimal levels of separation standard parameters be decided to maximize the system output?

Solutions for these problems and questions will benefit the passengers (for the controlled risks and delays), controllers (easier guidance and control mechanism), airlines (by higher customer satisfaction, higher safety, and more realistic planning), and the country (by better system utilization).

1.5 Methodology Overview

The first step to address these questions is to understand the uncertainty of the approach and landing process. This research models the uncertainty using probabilistic and statistical methods. Statistical analysis of aircraft landing track data is used as inputs to this study. We will address the questions using the following methodologies.

The answer to the first question is a direct output of the statistical analysis of aircraft landing track data. Theoretical estimations will be provided along with empirical ones.

The answer to the second question is necessary to answer the other questions. This dissertation suggests that the current *minimum separation* standards under Instrument Flight Rule, given in Table 1.1, should be replaced by statistical separation standards (SSS). SSS specifies a *target separation value* as an operational standard. In addition, it specifies a *lower specification limit* for the separation of any given pair and a standard for the *variance* of the process.

The optimal level of *target separation*, which defines the optimal level of the system output, depends on the cost of avoiding the *in-trail wake vortex hazard* and *runway incursion* risks, and the benefit gained from closer and more frequent landings. In this dissertation, we consider the cost and benefit as general terms either expressed in terms of landing frequency or dollar values.

To calculate the WV hazard and SRO risks for a given target separation, we obtain probability distribution functions (PDF) of:

- *aircraft spacing* in the common landing path when infinitely many aircraft are in the line to land
- Landing Time Intervals (*LTI*) to the runway threshold
- Inter-Arrival Times (*IAT*) at the final approach fix (*FAF*)
- Aircraft Runway Occupancy Times (*ROT*)

These probability distributions are to be calculated from samples extracted from aircraft time-position track data collected by the multilateration surveillance system in the vicinity of Detroit airport (DTW).

Imposed separation, corresponding to the first distribution, is not directly observable from aircraft track data. This study develops a method to obtain this probability distribution using distributions of the other variables. This dissertation does not consider probability distributions for the locations and strengths of wake vortices, although we discuss how these values should be employed to obtain minimum wake vortex safe

separation. They can be calculated using existing wake vortex models such as the Probabilistic Two Phase (P2P) model, the AVOSS Prediction Algorithm (APA), and the TASS-Driven Algorithm for Wake Prediction (TDAWP). In this research we provide a safe wake vortex separation threshold using the current separation probability distributions.

The study develops optimization models to maximize the system output (either the landing frequency or the dollar value benefit) given appropriate cost and benefit factors. The optimization is extended to include a given fleet mix. These models also provide frameworks to estimate the runway landing capacity taking into account the uncertainty of the landing process.

CHAPTER 2 LITERATURE REVIEW

This chapter summarizes the literature that is most relevant to this research. It is organized in a chronological order.

In a classical capacity study, Blumstein (1959) developed an analytical expression for the landing capacity (or service rate) of a single runway under IFR in which aircraft are restricted by a minimum space separation at the beginning of a common approach glide path and by a minimum time separation at the runway. He considered the realistic case where the velocity differences between successive aircraft exist. However, in all cases the velocity was assumed to be constant throughout the glide slope.

He defined runway landing capacity or service rate as the landing rate under conditions of saturated arrivals. To calculate the capacity, he considered a uniform distribution for the landing speed; however, the distribution is the same for all types of aircraft. In another extension he assumed different, but deterministic, speeds among the different aircraft types. He determined the landing rates for each of three New York area airports, i.e., Idlewild, LaGuardia, and Newark. He estimated single runway landing capacity about 30-40 landings per hour under IFR, one minute landing separation over the threshold, 10 nm common path, and 3 nm separation at the beginning of the common path, named the “gate”. The analysis indicated that the greatest capacity improvement is

derived from a reduction in the separation required at the gate. He suggested that since this separation is dictated largely by errors in knowledge of aircraft position, improvement can come with more precise position information by better radar and higher information rates. He demonstrated that landing rate decreases as the spread in velocity of the landing aircraft increases.

Lebron (1987) studied the potential increase in airport (runway) capacity that might be obtained from technical improvements in a single runway, dual parallel runways, and dependent parallel runways. He suggested that by reducing inter arrival time variability by 50%, landing capacity can be increased by 18% under VFR and 14% under IFR. A mix of arrivals and departures were considered. Both IFR and VFR were considered. No distributions were provided.

Vandevenne and Lippert (1992 and 2000) presented a model to represent *LTI* and provided a probability distribution fit. Their model was the convolution of an exponential and a normal distribution. They used *LTI* samples collected by B. Joss *et al*. at DFW. A continuous data recorder (CDR) was used. 42 samples of *LTI* for Large-Large aircraft at the Outer Marker were obtained, but the same distribution was also assumed at the threshold. The other set (Joss) contained 46 samples without heavy aircraft.

Ashford and Wright (1992) dedicated a chapter in their book to airport capacity and another chapter to airport safety. They listed factors affecting runway capacity as the following:

- Air traffic control factors including: separation (as the dominant factor), the length of the common path from the IFR gate to the threshold, the strategy used by controllers in sequencing aircraft traveling at different speeds (e.g., first come first served, or speed-class sequencing), the allowable probability of violation of the separation rule (acceptable risk level), and the sophistication of the air traffic control system (which affects the precision with which aircraft can be delivered to the IFR gate), and the ability to monitor aircraft speeds and detect aircraft positions and movements.
- Characteristics of demand in terms of aircraft size (and fleet mix), speed, maneuverability, and braking capability, as well as pilot technique. These affect the landing separation and runway occupancy time.
- Environmental conditions in the airport vicinity, wind direction, visibility, humidity, noise regulations, etc.
- The layout and design of the runway system
    - The number, spacing, length and orientation of runways
    - The number, locations, and design of exit taxiways
    - The design of ramp entrances

They categorize the procedures for estimating hourly and annual runway capacities as empirical approaches, queuing models, analytical approaches, computer simulation, and the FAA Handbook Approach. To estimate airport capacity, one needs to consider the gate and taxiway capacities as well.

Credeur et al. (1993) collect data to compare 3 FASA (final-approach spacing aids) display formats. They provide some empirical estimates for the communication times between pilot and controllers under VMC.

Gilbo (1993) points out that the most important and restrictive NAS component is the airport and the problem of predicting airport capacity is less resolved in comparison to air traffic demand forecast. He uses empirical (historical) data of runway operations to estimate arrival and departure capacity curve (Pareto frontier) of a single runway. He considered the ratio of arrivals to departures in the capacity calculation. The data are for major US airports from 1989 to 1991 represented in the Unisys interim memorandums. He uses the frequency of occurrences of extreme observations to eliminate extreme observations in order to increase the estimation accuracy. Using these curves as input parameters, he formulated some mathematical programming models to minimize the total landing and departure queue length given demand for every time unit.

Haest and Goverts (1995) addressed the contribution of radar plot accuracy to horizontal separation standards with the normality assumption for displayed polar coordinates on the radar screen.

Ballin and Erzberger (1996) statistically analyzed threshold time and space separation under high-demand arrival conditions at Dallas/Fort Worth International Airport (DFW). The primary goal was to obtain a reference baseline for the assessment of the CTAS (center TRACON automation system) as it is tested at the airport. DFW was scheduled to

be the first site for field testing of the FAST (final approach spacing tool) component of CTAS.

They used live radar track data recorded for a selected set of arrival rushes over a six months period consisting about 4450 aircraft separation pairs. Radar track data and additional supporting information were recorded at DFW and the Fort Worth Air Route Traffic Control Center (ZFW). Radar tracks of aircraft on final approach normally do not extend to the threshold, so the existing radar data were used to extrapolate aircraft flight-paths to the most likely runway (by using a Kalman filter). A comparison with tower observations showed the threshold crossing times to be accurate to within about 10 seconds. Data were split to identify IFR and VFR landing conditions.

Ballin and Erzberger evaluated aircraft landing rates and separations at DFW airport. They estimated unused / lost landing opportunities that occur during rush periods. The effects of variance reduction (through automation) on capacity were also studied at DFW. Mean rush rates were about 33, and 36 landings/h for IMC and VMC conditions, respectively, which also differed among different runways. They estimated the capacity based on target values not the average separation. They estimated the potential maximum achievable landing rates (capacity) using two different formulations. Given the arrival mix, the results indicated that the potential maximum landing rate was approximately 50 aircraft per hour for each runway. The other method gave 40 landings/h, which differed by 10 aircraft per runway per hour from the other method. These estimates were criticized as being very high by Hemm (1999).

Ballin and Erzberger analyzed 470 samples for 2.5 nm pairs (which were generally IMC with some VMC data). In 7.5% of the cases the 2.5 nm separation minimum was violated. The fitted smoothed PDF had a mode of 3.23 nm (90 sec), a mean of 3.93 nm (101 sec), a standard deviation of 1.23 nm (30.1 sec), and a median 3.66 nm (96 sec). They also analyzed 323 samples of 3 nm minimum separation pairs. They obtained 50 samples of 5 nm separation minimum pairs, with a median of 5 nm, a mean of 5.06 nm, a standard deviation of 0.95 nm, and a mode of 4.8 nm.

They did not fit a known PDF to the data but they did fit some smoothed distributions (not necessarily uni-modal) which provided a mode assumed to be the target separation. They mentioned the Vandevenne model but did not use it directly. They claimed to observe 16 to 48 landings per runway-hour during rush periods. They observed: 1) nearly identical separation distributions for 2.5 nm and 3.0 nm minima (under restrictions). 2) large numbers of negative excess required minimum separation and small target buffers for the higher required minimum separation cases, and 3) a very high incident of negative excess separations for aircraft following B757s.

Hemm *et al*. (1999) studied the possible benefits gained from implementing a Terminal Area Productivity (TAP) program. TAP includes the following subsystems:

1. RSO (Reduced Spacing Operation) including AVOSS and AILS,
2. LVLASO (Low Visibility Landing and Surface Operations) including ROTO, T-NASA, and DROM,

3. ATM (air traffic management) including CTAS (Center TRACON Automation System) and FMS (flight management system). CTAS includes TMA (traffic management advisor), P-FAST (Passive Final Approach Spacing Tool), A-FAST (Active Final Approach Spacing Tool), and DA.

They estimated benefits accruing from deployment of AVOSS, DROM, ROTO, and CTAS/FMS integration systems. The goal of AVOSS was to reduce the excess distance by providing controllers with more accurate wake-vortex threat information. They estimated significant benefits from AVOSS. They modeled two levels of CTAS/FMS integration (ATM-1 and ATM-2). They pointed out that the current (1999) position accuracy was 0.25 and was expected to reduce to 100 feet in 2005 by employing GPS technology. Active/Passive Final Approach Spacing Tool with a data link can exploit reduced uncertainties in aircraft speed and position to reduce separations. Benefits consisted of the minutes of the arrival delay saved by the TAP technologies at 10 major airports during a 10 year period from 2006 through 2015.

All the potential benefits of TAP were based on the confirmation of some key assumptions - for example, that DROM demonstrates average runway arrival times less than 50 sec in rain and that the flight plans produced by integrated CTAS and FMS computers can be safely accepted and executed by controllers and pilots.

Hemm *et al*. utilized the LMI (Logistics Management Institute) runway Capacity and Delay Models (Lee *et al*. 1997) for their study. We summarize LMI landing capacity model here. The capacity model algorithms include confidence factors of 95% for mile-

in-trail separation and 97% for single runway occupancy. These are standard values used in airport analysis and are applied for all technologies.

They derived a normal *IAT* distribution from V_L, V_F, D, and some variances of speed and wind effects. Normal distributions were considered for aircraft velocity, wind velocity, *ROT*, and aircraft position. The algorithm eventually derives a condition on separation at the TRACON gate (μ) so that

$$\Pr\{D - X_F(t_{LO}) \geq S\} \geq 0.95 \text{ and } \Pr\{SRO\} \leq 0.975$$

where X is the aircraft position, D is the length of the common approach path, generally between 5 to 12 nm, t_{LO} is the time that the leader crosses the threshold, and S is the mile-in-trail separation minimum. To calculate μ, it provides a linear approximation for *LTI*.

It obtains μ for two cases where the speed of the leading aircraft is less or more than the speed of its follower. A Poisson process is used to model the arrival process to the TRACON. Capacity is estimated based on expected accommodated per hour capacity 3600/mean(time). Hemm *et al*. obtained 30 arrivals per hour for a given example; however this reduced to 28 landings per hour after adding Poisson uncertainty to the arrival process. The report criticized the Ballin study by indicating that they have used low variability; their maximum capacities can not be achieved with the average reported velocities. Hemm *et al*. also utilize some LMI models developed to estimate delays and departure capacities.

Sherry *et al*. (1999) studied the efficiency of traffic flow in the TRACON with respect to CTAS and FMS (flight management system). Overall arrival performance of the TRACON was measured by the capacity to land aircraft safely. Variation in the trajectory of each aircraft contributed to the arrival queue length, time in queue of other aircraft and flying time to the runway. They indicated the sources of aircraft position uncertainty as follows:

- Hand-off location and initial speed of the aircraft (due to traffic volume)
- Actual position of the aircraft (due to radar surveillance errors)
- Predicted future position of the aircraft (due to the difference in airmass-reference and earth-reference)
- Limited time and authority to adjust the aircraft trajectory (Romahn 1999)
- Converting earth-referenced control strategies into airmass-referenced heading and speed instructions
- Delay and authority with which a given aircraft complies with controller instructions

The controller compensates for these uncertainties and limitations by using spacing buffers over and above the minimum required spacing. Variance reduction has benefited the least from introducing CTAS.

In recent years, multilateration systems have been installed in some airports, including Detroit Metropolitan Wayne County airport (DTW). These systems provide

reasonably accurate time-position estimates of all transponder-equipped aircraft (a/c) operating in the airport vicinity in all weather conditions. These data can be used to obtain samples of landing process variables, such as the Landing Time Interval (*LTI*) between successive aircraft to the runway threshold, the Inter-Arrival Distance (*IAD*) between two successive aircraft at the moment that the lead aircraft crosses the runway threshold, and Runway Occupancy Times (*ROT*). ROT is the length of time required for an arriving aircraft to proceed from over the runway threshold to a point clear of the runway. This research considers *LTI*, *IAD*, and *ROT* as (random) variables.

Andrews and Robinson (2001) analyzed landing data of DFW using 4,573 aircraft radar track data. They extended the capabilities used by Ballin *et al*. (1996). They fit probability distribution functions for *LTI* using the Vandevenne and Lippert (2000) model. They estimated the *LTI* probability distribution and runway utilizations. They compared *LTI* at the outer marker with that at the threshold and found their correlation to be 0.88. They also measured the *LTI* histogram for 1,758 landing pairs. They plotted the *IAD* histogram for 801 large-large pairs. They used the Vandevenne model in their analysis. Correlation between excess threshold landing time and distance was 0.84 for 198 arrival pairs. They suggested that capacity can be increased using a target separation of 72 seconds.

Haynie (2002) collected *LTI* and *ROT* data from landings on runway 26R at ATL, under VMC. He used a stop watch for his field observations. Haynie's data set included a total of 405 landing samples, 364 of which had measurements of both *LTI* and *ROT* with

a correlation coefficient of 0.011. Haynie also collected 584 samples (from which 126 were under IMC) from LGA in 2002. He also obtained 135 samples under IMC at BWI. He investigated the relationship between aircraft safety and the landing capacity of the near terminal airspace. He looked into the technical errors and human factors, the reduction in the safety level by reducing the separation spacing, and the use of new technologies to eliminate or reduce the unnecessary spacing.

Lang *et al*. (2003) studied the possibility of increasing throughput by using cross-wind information in sequencing the landings on closely spaced parallel runways. They studied the effect of safe reductions of wake vortex separainima. They added random values (from a uniform distribution) to the minimum separation to account for variability in spacing precision. They concluded that a capacity increase is possible by some procedural changes at some airports, i.e. LAX, SFO, SEA, CLE, STL, PHL, and BOS. For example, they estimated a 2.3 and 8.7 landings per hour increase in arrival capacity at LAX and BOS, respectively, under their suggested procedure among three analyzed procedures.

Levy *et al*. (2003) analyzed aircraft positional errors. The position error is represented by the TSE (total system error) which is a combination of the FTE (flight technical error) and the NSE (navigation system error). Their paper only focuses on the statistical analysis of FTE for aircraft flying straight, final approach segments. The purpose of data analysis of the lateral and vertical error is the ability to infer the probability that an aircraft remains within the lateral and vertical dimensions of the containment volume.

They fit Johnson curves to lateral and vertical error data. Their goal was to improve the accuracy of statistical analysis of FTE data by: 1) applying different PDF models, and 2) assessing the impact on cross-correlated tests due to autocorrelation in the lateral and vertical FTE.

Freville *et al*. (2003) showed the potential benefit of utilizing time-based separation instead of distance-based separation in headwind landing. This was also supported by Bruin (2006). Bruin went further and showed this benefit for steep decent landing approaches. He illustrated the results on Schiphol Airport.

Levy (ICNS 2004) used multilateration data of Memphis international airport (MEM) to estimate landing capacity under both IMC and VMC. They observed 14,252 arrivals in January 2003, 10,108 of which occurred under VMC and 4,144 under IMC. They considered a fleet mix of different landing pairs. The number of *IAD* and *LTI* samples of large-large pairs under IMC was 614 and 333, respectively. Their capacity simulation for the available fleet mix and uniform separation distribution function resulted in 26.5 landings per hour for a given fleet mix scenario. Their maximum arrival rates for the given fleet mix resulted in 37.0 landings per hour. Their maximum estimated rate is for the pairs Heavy-B757 as much as 49.2 landings per hour. They presented a regression model relating quarter-hour arrival rates to inter arrival time and distance spacing over the runway threshold.

Levy *et al*. (DASC 2004) used multilateration data of MEM to obtain probability distributions of *LTI* and average landing speed conditioned on the type of follow-lead

aircraft in visual meteorological condition (VMC). Their samples come from about 103,000 landing operations (in 197 days) from which about 90,000 had a known wake vortex weight class. They fit *IAD* with a Johnson distribution using 1,161 and 623 samples for regular (*LTI* less than 240 sec) and peak period (*LTI* less than 150 sec) traffic, respectively. They also estimated the distribution of landing speed using 1,161 pair aircraft samples. They did not differentiate data on the B757. For large-large they obtained an average *IAD* of 3.8 nm in push traffic and 4.6 in regular times. The average speed was 133 knots for large-large pairs. Then using these distributions they estimated the capacity by stochastic simulation. In the author's point of view, their criteria actually did not indicate rush periods but rather indicated close-distance landings. Using the obtained distributions and fleet mix, they simulated the system throughput. The average throughput in a rush period was 30.1, 28.8, and 25.0 landings per hour for small, large, and heavy aircraft, respectively. The airport average was 27.7 landings per hour.

Rakas and Yin (2005) used the Performance Data Analysis and Reporting System (PDARS) database to estimate the probability distribution of *LTI* under VMC in Los Angeles International Airport (LAX). For this purpose, they developed a PDF named a *double-normal* distribution. Their sample included 1,516 *LTI* observations. They also referred to the Vandevenne model to analyze the *LTI* characteristics.

Xie (2005) provided distribution fits for Haynie's observations on ATL, as well as his own field observations from LaGuardia airport (LGA). However, the sample sizes were small, and the results were not conditioned on aircraft weight class types, or heavy traffic

times. Also, they have not obtained samples of *IAD*, which are provided in this dissertation.

Xie collected 245 *LTI* samples under VMC, and 150 *ROT* samples. One case of SRO was observed. Haynie's ATL mean *LTI* was 96 sec and Xie LGA mean was 103 sec. Xie noted that the *LTI* mode observed at ATL was 10 seconds larger than that of the LGA data.

Xie noted that Haynie's ATL 2002 *LTI* data had a mixed normal distribution, i.e., 38.5% of $N(67.2,10.4^2)$, 48.6% of $N(94.6,19.7^2)$, and 12.9% of $N(180.2,66.3^2)$. The expectation maximization (EM) method was used to obtain this fit. He fit a mix of three normal distributions to his own LGA 2005 data, as 70.8% of N(88.7,16.5), 28% of N(128.2,40.7) and 1.2% of N(274.6,16.1). He estimated $ROT \sim N(36,6^2)$ then calculated Pr{SRO}~=0.0042. In his field sampling, Xie observed one SRO out of 245 landings at LGA, thus P{SRO}~=0.005.

Using confidence interval formulations for rare events he provided 95% confidence interval for P{SRO}. His estimates were $[7*10^{-5}, 0.015]$ for Haynie's ATL samples (while the FAA LGA 2002 estimate is $4.5*10^{-6}$) and $[1.03*10^{-4}, 0.0227]$ for LGA samples (while the FAA estimate is $5.4*10^{-6}$). Thus, for both airports, the FAA report is under estimating P{SRO}.

CHAPTER 3 STATISTICAL CHARACTERISTICS OF THE LANDING PROCESS

Understanding the stochastic behavior of the approach and landing process is critical to analyze runway separation risks, throughput, and capacity. This dissertation applies statistical analysis for this purpose. This chapter deals with empirical and theoretical estimates of the critical random variables of the landing process, i.e., *LTI*, *IAD*, and *ROT,* and will estimate the current level of risk (or safety) and throughput in the landing process.

3.1 Background

A summary of previous statistical studies is given in Table 2.1. Levy *et al*. (2004) use multilateration data of Memphis International airport (MEM) to obtain probability distributions of *LTI* and average landing speed conditioned on the type of follow-lead aircraft in visual meteorological condition (VMC). Probability distributions for *LTI* and *ROT* are also estimated by Haynie (2002) for Atlanta International airport (ATL) using his field observations from this airport. Xie *et al*. (2003, 2004, and 2005) provide distribution fits for Haynie's observations, as well as his own field observations from LaGuardia airport (LGA). However, the sample sizes are small, and the results are not conditioned on aircraft weight class type, or heavy traffic times. Also, they have not

obtained samples of *IAD*, which we provide here. Ballin *et al*. (1996) provides analysis of *IAD*, *LTI*, and runway utilization in peak periods at Dallas/Fort Worth International Airport (DFW). They include both instrument meteorological condition (IMC) and VMC times in their study; however, they do not fit known specific probability distributions to the observations.

Vandevenne and Lippert (1992) develop a model to represent *LTI* and provide a probability distribution fit. This model is the convolution of exponential and normal distributions. Andrews and Robinson (2001) extend the capabilities used in Ballin *et al*. (1996). They fit probability distribution functions for *LTI* using the Vandevenne and Lippert model. Rakas and Yin (2005) use Performance Data Analysis and Reporting System (PDARS) database to estimate probability distribution of *LTI* under VMC in Los Angeles International Airport (LAX). For this purpose, they develop a PDF which they call a *double-normal* distribution.

The Center for Air Transportation Systems Research (CATSR) at George Mason University (GMU) has access to multilateration surveillance system data of DTW via Volpe National Transportation Systems Center, an organization within the US Department of Transportation. The original multilateration data are de-identified by Sensis Corporation, and the filtered data are used in this study. However, as discussed later, there are still some outliers, noise, and missing data present in the database.

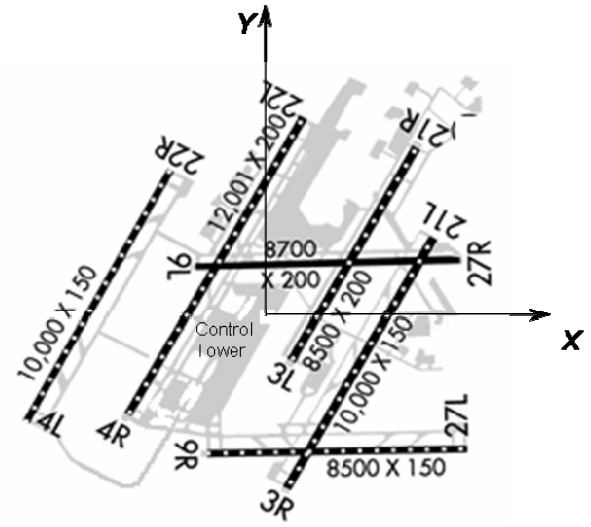

Figure 3.1. Simplified DTW airport diagram (FAA 2006)

3.2 Data Analysis and Distribution Fitting

This section introduces the characteristics and organization of available data and the algorithms that we have initiated to extract some specific recorded data. These data include aircraft times over the FAF (final approach fix), landing time/position over the runway thresholds, runway exit times, and the position of the following aircraft when the leader crosses the runway threshold. This algorithm is used to investigate aircraft data at DTW on Dec. 2002, Feb. 2-8 of 2003, June 2003, and August 2003 (in Greenwich Mean Time) in order to provide probability distributions for *IAT* (inter arrival time) at the final approach fix, *LTI* and *IAD* at runway thresholds, and *ROT*. The data of Dec 2002, June 2003, and Aug 2003 on runway 21L were pre-processed by Vivek Kumar in CATSR which makes the data ready to be directly feed into MATLAB algorithm which is discussed later in this section. Figure 3.1 is a simplified diagram of this airport.

3.2.1 Database Structure and Sample Extraction Procedure

Multilateration data must be processed to perform probabilistic analysis of the operations. There are two categories of short comings with the data. First, the data contain noise, outliers, and missing records, and second, the data provide the aircraft time-position tracks but do not specify when aircraft cross certain positions. In this section, we discuss these problems and explain our strategy to extract necessary samples for statistical analysis of the approach process.

We make use of five fields from the multilateration data (out of a possible eighteen): aircraft mode-s, time (t in seconds), horizontal position X in meters (along the longitude), vertical position Y in meters (along the latitude), and mode-c. The mode-s field is a number of an attached transponder that uniquely identifies an aircraft. The transponder is generally attached somewhere close to the center of the aircraft. The mode-c field is a barometer-based value that can be converted to altitude (in feet) by multiplying it by 25 and adding 10,000 to the result. However, the obtained value is not very reliable for this purpose due to pressure change and barometer errors for different weather conditions. Time and position of aircraft are meant to be recorded for every second. For the week Feb 2, 2003 to Feb 8, 2003, the database includes 33,030,878 records for all runways, requiring 1GB of disk space.

3.2.2 Data Preparation

The database is in Oracle format and we use SQL+ to obtain queries. Necessary manipulations and sample extractions are done in MATLAB. To start, we sort the Oracle

data by mode-s and then by time. We also change the time stamp to the format "dd/mm/yy hh:mi:ss." Basic queries demonstrated that the mode-s is missing for some records. In some cases, the mode-s of an entire aircraft track is missing. In other cases, we are missing the mode-s of only a few points along a track. We eliminate all of these data points. In the latter case, we retain the basic track path, since we can linearly interpolate the path of the aircraft from the other points with mode-s. In the former case, we discard the entire track. This may result in some inter-arrival times that are too long. However, because of the available data, losing some possible landing records does not significantly influence the study.

In the database, the origin (X=0,Y=0) of the Euclidian coordinate is the FAA control tower located between runways 21R and 22L, as shown in Figure 3.1, and the y-axis indicates the true north. Runway 21L, and all other runways parallel to it, have a Magnetic angle of 214.8^o. True North and Magnetic North have an angle of 6.1^o W, as indicated in airport diagram (FAA 2006). Thus, the true angle of runway 21L is 214.8 – 6.1 = 208.7^o, or equivalently 61.3^o from the x-axis. Since data are collected in the true coordinates, we observe the same results by tracking the aircraft course on the runways (Jeddi 2004). In the same manner, we calculate the true angle of runways 27L/09R and 27R/09L as 1.3^o from the x-axis.

To simplify working with the database, we rotate coordinates to make the runways parallel to the x-axis. To find the aircraft position in the rotated coordinates we multiply the observed (x,y) position by the rotation matrix R as

$$R = \begin{pmatrix} \cos\alpha & \sin\alpha \\ -\sin\alpha & \cos\alpha \end{pmatrix} \tag{3.1}$$

where *a* is the rotation angle which is 61.3° for runways 21L/03R, 21R/03L, 22L/04R and 22R/04L, and 1.3° for runways 27L/09R and 27R/09L as described before. That is, the aircraft position in the rotated Euclidian coordinates is

$$\begin{pmatrix} X_r \\ Y_r \end{pmatrix} = R * \begin{pmatrix} X \\ Y \end{pmatrix}. \tag{3.2}$$

Using the rotation formula (3.2), we also transform the runway coordinates to the new coordinates.

Preliminary queries and plots demonstrated some noise in the data. Figure 3.2 is the ground projection (bird's eye view) of the track plot of sample aircraft landings on runway 21L. The lower figure is drawn to scale, whereas the upper figure is expanded in the *y*-axis. In the figure, two aircraft exit the runway from the high-speed exit located after the middle of the runway. Based on visual investigation, the noise of (*x,y*) positions is assumed to be in an acceptable range, for a given time, as demonstrated in the lower part of Figure 3.2. In frequent cases, there are two or more records of a given aircraft at the same second. We average the records in such cases.

Table 3.1. Number of peak time landings observed; Feb. 2-8, 2003

	Runway													
a/c Type	**03L**	**03R**	**04L**	**04R**	**09L**	**09R**	**21L**	**21R**	**22L**	**22R**	**27L**	**27R**	**Total**	%
Not Available	-	1	3	-	-	-	11	0	0	7	1	2	26	1.4
Small	-	19	26	-	-	-	98	0	3	101	18	17	280	15.1
Large	-	96	158	-	-	-	445	1	18	483	107	111	1418	76.2
B757	-	8	15	-	-	-	39	0	0	51	5	11	129	6.9
Heavy	-	0	4	-	-	-	1	0	1	1	0	0	7	0.4
Total	**0**	**124**	**206**	**0**	**0**	**0**	**594**	**1**	**22**	**643**	**131**	**141**	**1862**	**100**

Since landings are the subject of the study, it is sufficient to consider data in a rectangle, which we call the "query box." The sides of the query box are parallel to the sides of the runway rectangle, and the box includes the runway and the common landing path extended about 10 nm from the runway threshold. For runway 21L, for example, we consider the rectangle -1350m$<X_r<$18500m, and -3000m$<Y_r<$-800m. Figure 3.2 illustrates that data beyond this rectangle are dropped from the query. We obtained queries for every runway for the entire week. We transform the time stamp of each of these outputs to second-format with respect to a time reference. We consider 12 am on January 1, 2003 as time zero.

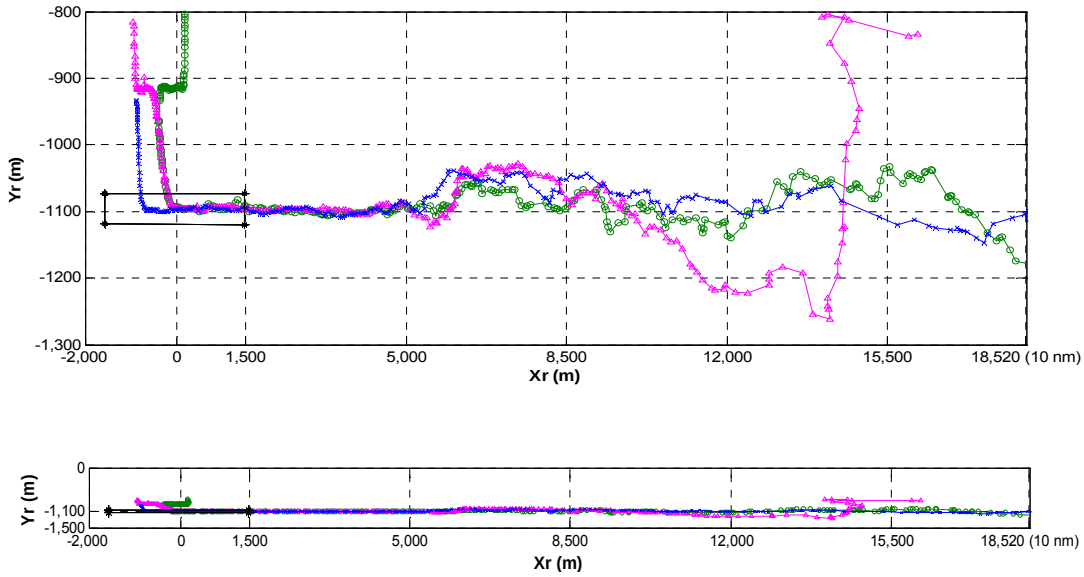

Figure 3.2. Landing and exit tracks of three large aircraft on 21L

Position is recorded at a second rate; however, there are time gaps when position is not recorded. For such cases, if the gap is at most 10 seconds, we linearly interpolate the time-position of the aircraft between two boundaries of the time gap for every second. We do not apply this interpolation for the time gaps of more than 10 seconds. This procedure is implemented in MATLAB.

This procedure is applied to the outputs provided by Kumar and Shortle. They have extracted landing data on runway 21L at DTW form multilateration data. The track data are averaged on a one-second basis. I have applied the interpolation procedure to fill up the existing gaps in their output.

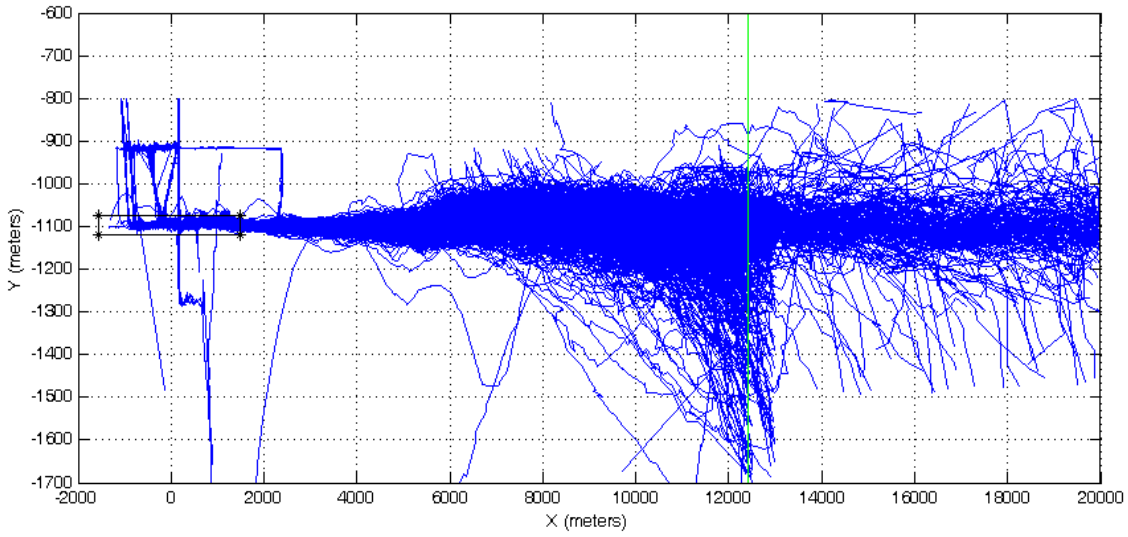

Figure 3.3. Landings on runway 21L (scale of Y-axis is distorted)

From the plotted tracks in Figure 3.3, it is seen that some landings follow an approach course parallel to the *y*-axis toward the FAF. Then they cut the corner once they are about 0.5 nm from the FAF and turn toward 21L. This dissertation does not focus on these landings and mainly focuses on landings that are in the 21L direction while crossing the FAF; see Appendix for the exact FAF position. All the collected information is conditioned on these landings in this report. (In the early stages of this study we considered all landings on all runways of DTW for the week Feb. 2-8 of 2003 under IMC. We have reported the statistical outputs of the early studies in Jeddi *et al*. 2006.)

The total number of analyzed landings on runway 21L during four different months is 1402. We only study the last two weeks of December 2002, the first week of February 2003, and June and August of 2003. For some days in these periods, we observe no landings on runway 21L. This might be because on these days either aircraft land on

other runways or the data are not collected, for any reason. We condition these landings on approach direction and peak periods as described later in this section.

We also need to verify the information about wake vortex weight classes, and weather conditions (Instrument Meteorological Condition IMC or Visual Meteorological Condition VMC), and add it to the track data. We have obtained the wake-vortex weight class of 96% of the landings under study, of which 67% are provided by Sensis Corporation and the rest are obtained by matching and search of tables of the FAA aircraft registration database, including MASTER, ACFTREF, and Aircraft Information tables. The weather condition for every quarter hour is reported in the ASPM (Aviation System Performance Metrics) database in local time. Considering the time column of the data, we add a new column to indicate IMC and VMC weather condition. We assume that all landings under IMC condition follow Instrument Flight Rule (IFR).

After data preparation in the aforementioned manner, we now discuss how to extract samples of random variables of the landing process, and compute desired landing statistics. Recorded data of a given aircraft might include many landings, departures, or fly-overs, but these operations are not differentiated in the database. We now introduce an algorithm to distinguish landings from other operations, and to calculate samples of *LTI*, *IAD*, and *ROT* samples.

3.2.3 Algorithm to Extract Samples

The following procedure recognizes landings then extracts necessary records for subsequent statistical analysis:

1. For each mode-s, divide all records of a single aircraft into separate operations (landings, departures, etc). We suppose that a new operation begins whenever there is a time gap of more than 15 minutes between any two records of that aircraft. Any of these operations might be a landing, departure, fly over, or a ground operation.
2. Check if a given operation is a landing on a given runway, 21L for example, by checking if it passes the following tests:

   - Let $t_{\min}$ and $t_{\max}$ be the first and last times for which the aircraft is in the "query box."
   - If $X(t_{\min}) - X(t_{\max}) > 5{,}000$ m, then the aircraft proceeds from right to left, and has been long enough in the runway direction to be a candidate for a landing on runways 21L, 21R, 22L, 22R, 27L, or 27R. Similarly, if $X(t_{\min}) - X(t_{\max}) < -5{,}000$ m, then it is a candidate for a landing on runways 03R, 03L, 04R, 04L, 09R, or 09L.
   - Check if the aircraft ever crosses the threshold of the specific runway and is observed over the runway.

3. Repeat step 2 for all operations and aircraft, and record their threshold time and location. Record the time and location of aircraft when it is first observed outside of the runway rectangle after landing, i.e. taxi-in time and location. If the aircraft track disappears over the runway, then the exit from runway is not recorded, record zero or blank for the exit time.

4. Sort landings in ascending manner, to recognize follow-lead aircraft. Record the location of any follow aircraft at the moment its lead crosses the runway threshold.
5. Calculate *ROT* for any aircraft, and *LTI*, and *IAD* for any pair of lead-follow aircraft.

Depending on the objective of a study, observations shall be classified based on weather condition, weight class of follow-lead aircraft, arrival rate, etc.

3.3 Landing Statistics

We define a peak period for a given runway to be a quarter-hour with at least seven landings on that runway. For the week Feb 2, 2003 to Feb 8, 2003, for example, we observed 1,862 peak period landings out of 4,313 landings observed for the entire week on all twelve runways. For all studied data, we have observed 14,302 landings on runway 21L, including one week of February 2003.

Table 3.2. Total number of landing samples on runway 21L

a/c Type	Dec 2002	Feb 2003	June 2003	Aug 2003	Total	%
Not Available	7	8	33	133	181	3.9
Small	88	70	120	342	620	13.4
Large	367	318	720	2148	3553	76.5
B757	30	33	50	168	281	6.0
Heavy	2	0	1	9	12	0.3
Total	**494**	**429**	**924**	**2800**	**4647**	**100.0**

The total 4,647 landings in peak periods are distributed among runways and aircraft

types as shown in Table 3.2. The majority of these landings occur on runways 21L and 22R. Only 3.9% of wake vortex weight classes of peak period landings could not be recognized.

To validate if we are observing almost all landings in 15 minute periods (among those periods where the observed landing rate is positive), we focus on one week data of February 2003 and compare it with the recorded landings on all runways in ASPM database for this specific week of operations.

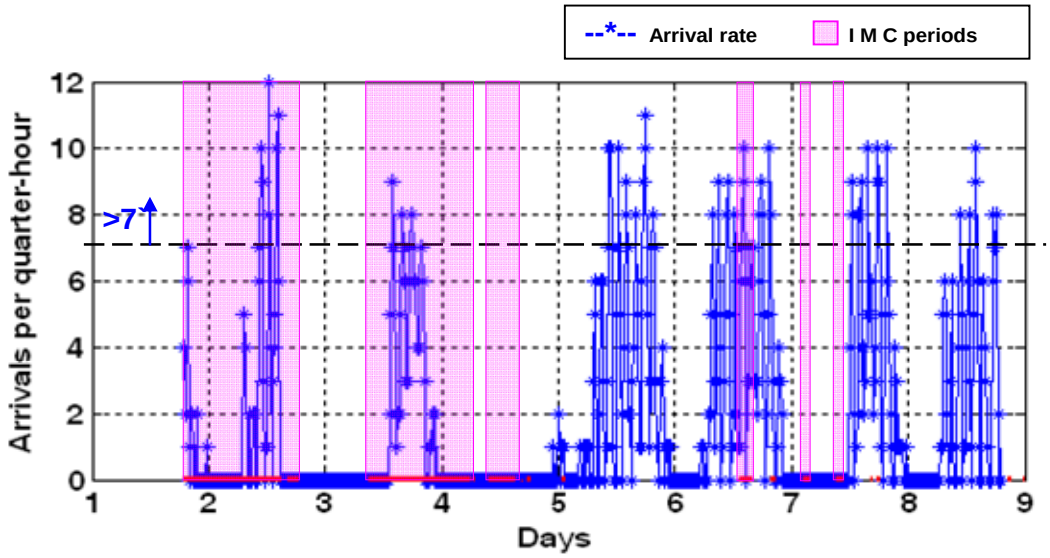

Figure 3.4. Arrival rate to runway 21L; Feb. 2-8, 2003, local time

Figure 3.4 shows arrival rates per quarter hour for runway 21L. The horizontal axis is in local time. Observations start at 7:00pm Feb 1, 2003. Shaded periods over the time axis indicate IMC periods for the airport. The arrival pattern for runway 22R is similar to this one since the arrival traffic is equally directed to these two parallel runways whenever these runways are in the landing configuration.

To double check the completeness of observations in the multilateration database and to validate our data preparation and sample extraction algorithm, we compared the number of landings reported in ASPM database with the results from our study. The comparison plot is given in Figure 3.5. Overall for this week, ASPM reports 160 more landings than ours. This corresponds to a small proportion of 3.6% (=100*160/4473) of ASPM records. Average and standard deviation of "Observed minus ASPM" rates are 0.24 and 1.7 arrivals per quarter-hour, respectively. This difference can be the result of missing mode-s and unrecorded landings that might have happened because of off transponders or non-transponder aircraft.

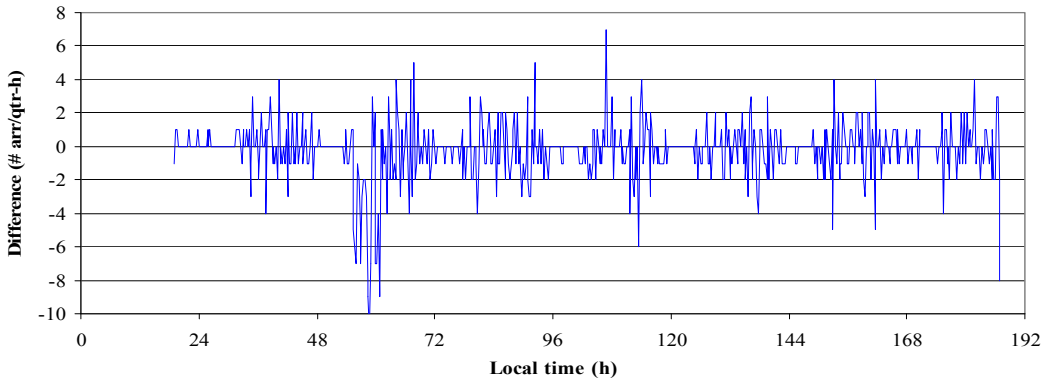

Figure 3.5. Arrival rate (observed minus ASPM) per quarter hour in Feb 2-8, 2003

To analyze system operations it is also important to know the proportion of follower-leader aircraft pairs. Table 3.3 shows this proportion for our data (peak times only), which is also called a transition matrix. About 59% of the pairs are large-large.

Table 3.3. Follow-lead aircraft transition matrix in peak periods; Feb. 2003 data

Follow \ Lead	Small	Large	B757	Heavy	Total
Small	1.7	12.5	1.2	0.1	15.5
Large	12.8	58.8	5.4	0.3	77.3
B757	0.9	5.4	0.6	0.0	6.9
Heavy	0.1	0.3	0.0	0.0	0.4
Total	15.5	77.1	7.1	0.3	100

3.4 Peak Period *IAT*, *LTI*, and *IAD* Probability Distributions

In risk and capacity analysis, the pattern of the approach process behavior in peak periods is of interest. For this reason, we focus on periods during which there are seven or more landings per quarter hour. We assume that under IMC, aircraft land under IFR (instrument flight rules) at DTW.

Table 3.4 shows the default standard for the "approach in-trail threshold separation minima" under Instrument Flight Rule (IFR) put forth by the FAA. We are interested to know what the probability distributions of *LTI* and *IAD* are for class of follow-lead aircraft with the 3 nm separation spacing minima indicated in Table 1.1, i.e. pairs S-S, L-S, B757-S, H-S, L-L, B757-L, and H-L. In specific situations, 3 nm spacing standard may be reduced to 2.5 nmi (FAA 1993). However, differentiating these situations is not the subject of this paper.

Table 3.4. IFR approach in-trail threshold separation minima (nmi)

Follow a/c	Lead a/c			
	Small	Large	B757	Heavy
Small	3	4	5	6
Large	3	3	4	5
B757	3	3	4	5
Heavy	3	3	4	4

We have collected a significant amount of samples on the variables of interest under IMC and VMC, i.e., Inter Arrival Time *IAT* at FAF, for 3 nmi pairs, *LTI*, and *IAD* at the runway threshold for 3 nmi and 4 nmi pairs. The number of samples, minimum value, maximum value, mean and standard deviation of the samples for each variable are given in Table 3.5 under IMC and Table 3.6 under VMC.

Table 3.5. Estimated landing distributions under IMC

IMC Variable	n	[min,max]	mean	Std	Fitted PDF	shift	scale	shape
IAT3 at *FAF*	772	[53,218]	105	30.7	Log-Logistic	50	48.45	3.46
LTI 3	770	[48,216]	104	30.5	Log-Normal	40	4.06	0.45
					Log-Logistic	45	52.30	3.60
IAD 3	752	[1.9,8.0]	3.6	1.0	Log-Logistic	1.8	1.50	3.30
IAT 4	162	[65,250]	121	35.5	Log-Logistic	60	53.84	3.25
LTI 4	162	[70,243]	124	32.2	Log-Normal	60	4.05	0.47
					Log-Logistic	65	53	2.57
IAD 4	152	[2.4,9.5]	4.1	1.1	Log-Logistic	1.3	2.60	5.36

Independence of the samples is necessary to fit probability distributions. Independence of samples is examined by "one-lag scatter plot" in Figure 3.6 for *LTI* of 3 nm. See Bowker and Liberman 1972, and Hollander and Wolf 1999 for more information on statistical concepts discussed in this chapter. The plot does not demonstrate a specific pattern of dependency among the samples, and on the other hand the one-lag and two-lag correlation coefficients of the samples of this variable are 0.15 and 0.08 respectively.

Thus we accept independence of *LTI* samples. In the same manner, we conclude independence of samples of other variables by examining the one-lag scatter plot and the correlation coefficients.

Table 3.6. Estimated landing distributions under VMC

VMC Variable	n	[min,max]	mean	Std	Fitted PDF	shift	scale	shape
IAT3 at *FAF*	1618	[40,236]	102	32	Log-Logistic	39	55.84	3.78
LTI 3	1623	[40,233]	101.5	32.2	Log-Logistic	39	55.30	3.80
IAD 3	1537	[1.5,7.3]	3.45	0.96	Log-Logistic	1.5	1.74	3.82
IAT 4	331	[48,231]	116.3	29.8	Log-Logistic	45	66.40	4.13
LTI 4	336	[56,238]	120.8	31.4	Log-Logistic	50	65.44	4
IAD 4	306	[1.6,7.0]	4.05	0.93	Log-Logistic	1.7	2.23	4.24

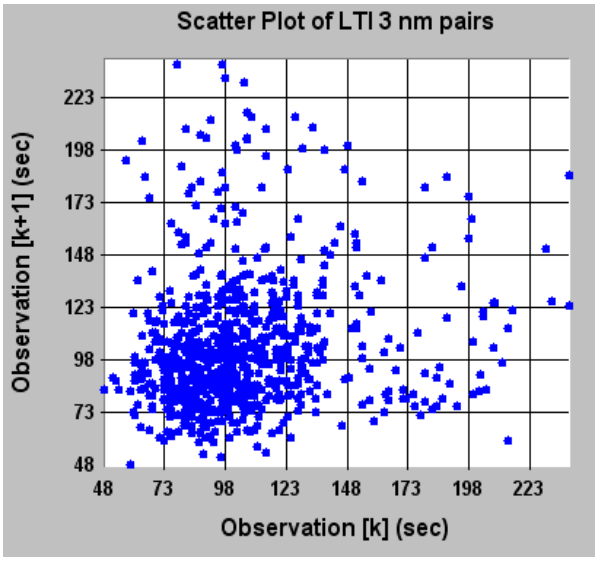

Figure 3.6. One-lag scatter plot of peak-IMC period *LTI* of 3 nm pairs

The summary of one-lag and two-lag correlation for variables of interest under IMC are given in Table 3.7.

Table 3.7. One-lag and two-lag correlation coefficients for the variables under IMC

Lag	Correlation						
	IAT3	*IAT4*	*LTI 3*	*LTI 4*	*IAD 3*	*IAD 4*	*ROT*
1	0.12	0.16	0.15	0.16	0.13	0.04	0.05
2	0.04	0.001	0.08	0.01	0.10	0.02	0.04

Figure 3.7 provides histogram and fitted probability distribution functions (PDF) for *LTI3* under IMC. The fitted distributions for all variables of interest are given in Tables 3.5 and 3.6 under IMC and VMC, respectively. Interestingly, for all of the variables, the shifted log-logistic distribution provides the best fit. However, for simplicity in some calculations, we will use lognormal distribution fits of *LTI3* and *LTI4* in chapter 5. The method of Maximum Likelihood Estimation (MLE) is used for these estimations.

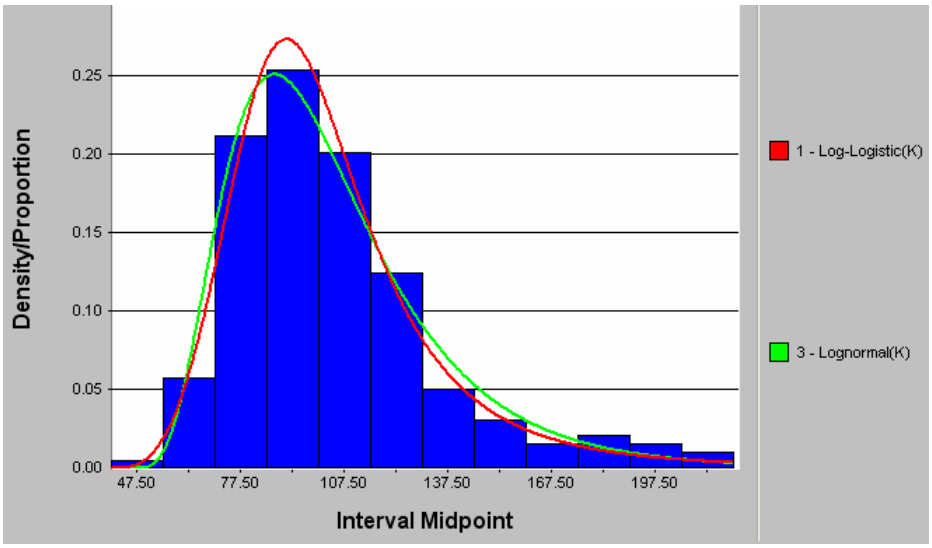

Figure 3.7. Histogram and distribution of peak period *LTI* 3-nmi under IMC

As given in Table 3.5, we have estimated the probability distribution of *LTI3* by lognormal(40;4.06,0.45) when we enforce a minimum of 40 seconds. Here, 40 is the *shift* parameter, and 4.06 and 0.45 are *scale* and *shape* parameters, respectively. The log-

logistic(45;52.3,3.6) distribution provides a slightly better fit than the lognormal distribution. The fit is accepted by a KS-test for significance levels of 0.05 or smaller.

Figure 3.8 provides histogram and distribution fits of *LTI4* under VMC. The Parameters of the fits are given in Table 3.6.

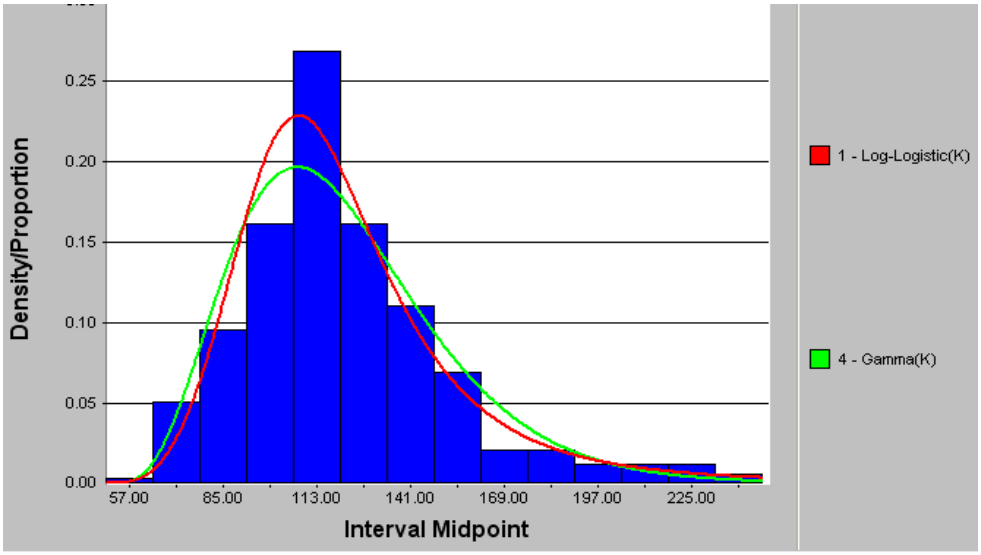

Figure 3.8. Histogram and distributions of peak period 4-nmi *LTI* under VMC

3.5 Estimation of Runway Occupancy Time

To estimate the risk of simultaneous runway occupancy, we need to estimate the probability distribution of the *ROT*. As we see from the airport diagram, 21L has 4 speed exits, two of which are prior to the half-way point of the runway and two others close to the end of the runway. This suggests that some proportion of the aircraft exit early and some exit later. This is also supported by the histogram of *ROT* samples of small and large aircraft, representing landings of leading aircrafts of 3 nm pairs in Table 3.3. We

condition the data on early exits and late exits. We observe that 59% of the landings exit early and 41% exit late. We fitted the early exits by beta(11.8, 27.9) in the range [20, 90] and late exits by beta(9.0,16.6) in the range [30, 110]. Thus,

$$ROT \sim 0.59\ \text{Beta}([20,100],11.8,\ 27.9) + 0.41\ \text{Beta}([30,120],\ 9.0,\ 16.6)$$

for the mix of small and large aircraft, i.e. aircraft pair 3 nm. This distribution is plotted in Figure 3.11. The Beta distribution might be preferred because, as in real situations for *ROT*, it has lower and upper bounds. For both the early and late exits, the normal distribution, which is used by some researchers for example Xie 2005, is rejected in the 0.1 significance level. The normal distribution remains to be a relatively valid estimation with a lower accuracy. The mean and variance of beta(*L, U; α, β*) are

$$\begin{cases} \mu = \mathrm{L} + (U - L)\cdot\dfrac{\alpha}{\alpha+\beta} \\ \sigma^2 = (U-L)^2\cdot\dfrac{\alpha\cdot\beta}{(\alpha+\beta)^2(\alpha+\beta+1)} \end{cases}.$$

Thus, the mean of the first and second parts are 41 s and 58 s, respectively. The overall mean is 48 s. For the mix of Large, B757, and Heavy aircraft, the distribution is slightly different from the previous case. As expected more aircraft exit later.

$$ROT \sim 0.567\ \text{Beta}([25,90],6.87,\ 21.8) + 0.433\ \text{Beta}([32,100],\ 7.39,\ 11.46)$$

The mean of the first and second parts are 40.2 s and 58.7 s, respectively. The overall mean is 48.2 s. The *ROT* might be better fitted using a 4-modal beta distribution by conditioning on the used exit. For this research, bimodal is sufficiently accurate.

We are also interested to know if *ROT* is different under IMC and VMC weather conditions. We have done some comparison using the one week data of Feb 2003. Figure 3.9 shows histograms of *ROT* under VMC and IMC for the runways with similar taxiway configurations, i.e. 21L/03R and 22R/04L. The structure of runways 27L and 27R seems to be different from 21L/03R and 22R/04L, as the *ROT* on these runways demonstrate, see Table 3.8.

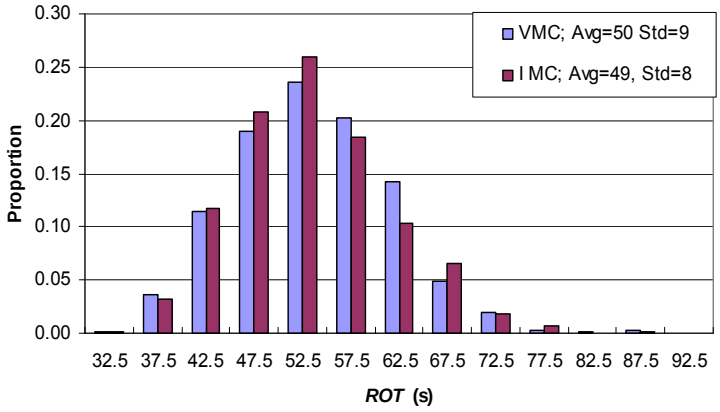

Figure 3.9. *ROT* under VMC (895 samples) vs. IMC (590 samples); Feb 2003 data

Visual inspection of Figure 3.9 does not suggest any significant difference between IMC and VMC *ROT* for this week of data. (Here, IMC/VMC is only distinguished by the corresponding flag in the ASPM database. We have not conditioned on other complementary variables, like surface visibility, which might also affect *ROT*. Thus, data from a different week in which surface visibility is reduced might show a distinction between IMC / VMC.) From the data, the average and standard deviation of *ROT* in VMC are 50 s, and 9 s, respectively. In IMC, the average and standard deviation are 49 s,

and 8 s.

Table 3.8. *ROT* in peak periods for landing runways; Feb 2-8, 2003 samples

Runway	Statistic	VMC	IMC	Runway	Statistic	VMC	IMC
03R	*n*	60	30	22R	*n*	283	171
	Range (s)	[33,68]	[32,64]		Range (s)	[26,72]	[39,70]
	Avg (s)	48	47		Avg (s)	53	50
	Std (s)	7	8		Std (s)	6	6
04L	*n*	63	91	27L	*n*	60	38
	Range (s)	[40,60]	[39,68]		Range (s)	[38,58]	[39,60]
	Avg (s)	48	49		Avg (s)	48	48
	Std (s)	6	6		Std (s)	5	5
21L	*n*	271	148	27R	*n*	72	26
	Range (s)	[31,70]	[29,72]		Range (s)	[38,105]	[36,84]
	Avg (s)	45	48		Avg (s)	57	54
	Std (s)	8	10		Std (s)	12	11
22L	*n*	22	-	**Total**	*N*	828	504
	Range (s)	[40,79]	-		Range (s)	[26,105]	[29,84]
	Avg (s)	55	-		Avg (s)	49	49
	Std (s)	9	-		Std (s)	8	8

3.6 Estimation of SRO Probability

We estimate the risk of SRO by the probability (or frequency) that the *LTI* between two consecutive aircraft is less than the *ROT* of the leading aircraft. We represent this probability by $P\{LTI_{k,k+1} < ROT_k\}$, k=1, 2, …. This is the runway-related approach risk.

Figure 3.10 shows pairs of observations ($LTI_{k,k+1}$, ROT_k) which is the *ROT* of the lead aircraft k versus the *LTI* between aircraft k and k+1 for peak period landings. This is the plot of one week Feb 2003 samples. We have limited *LTI* in the figure to 200 seconds

for the purpose of clarity. In this figure, pairs of follow-lead aircraft are not differentiated based on their weight class. For three points above 45 degree line, $LTI_{k,k+1}$ is less than ROT_k one of which has occurred under IMC. In this figure, there are two observations having *ROT* of 105 s which correspond to landings on runway 27R in VMC. They are exceptional cases since they are far from other sample population and we consider them as outliers. They are 19 s bigger than the second largest sample 86 s, for example.

Figure 3.10 also demonstrates independence of $LTI_{k,k+1}$ and ROT_k for all k. The Kendall "sample-correlation statistic," which measures dependency in non-parametric statistics, is 0.085 and supports independence of these random variables; for more discussion on this parameter see Hollander and Wolf (1999). The sample correlation coefficient is 0.15 and also confirms the independence hypothesis.

Now we provide an empirical and a theoretical "point estimate" for $P\{LTI_{k,k+1} < ROT_k\}$, k=1, 2, …, in peak periods for pairs of aircraft with separation standard 3 nm in Table 3.3. The estimate is obtained by using all 4,466 peak period samples explained in Table 3.2, conditioned on IMC periods.

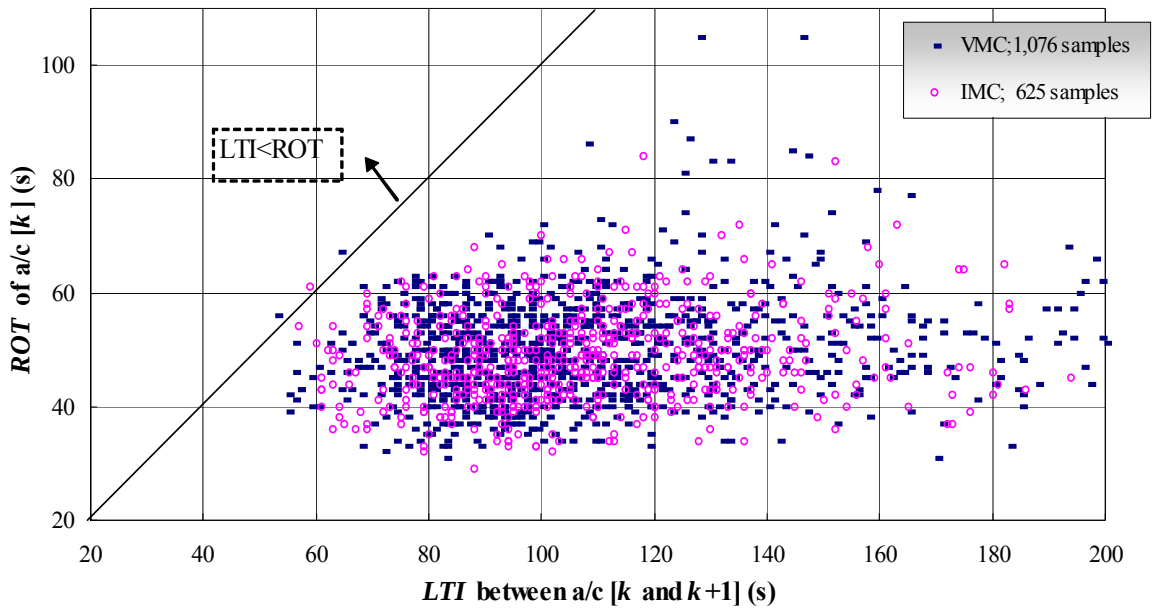

Figure 3.10. *ROT* of aircraft *k* versus *LTI* between aircraft *k* and *k*+1; Feb 2003 data

3.6.1 Empirical Method

There are totally 14 points where $LTI_{k,k+1} < ROT_k$, i.e. above the 45 degree line. The sample frequency is 0.0021 with respect to 6,832 peak period landings. There were some landings for which we could not obtain the *ROT* due to disappearance of the aircraft track over the runway. This might be because the aircraft turned off the transponders or for other reasons. We assume that these landings would not have been above the 45 degree line in the figure. On the other hand, multilateration data do not provide all the landings because of the errors in recording and off transponders. Thus, these estimations are optimistic, i.e., lower estimated risks.

We can also build a confidence interval using the observations. Assuming the

occurance of SRO as a rare event, the process of its occurance can be considered as a Poisson distribution. Then the 95% C.I. for SRO on this runway, under IMC, is [0.0011,0.0034]. If we condition SRO to the ones equal to or greater than 3 seconds, then we will have 6 SRO, and the point estimation will be 0.0010 and the 95% C.I. will be [0.0003,0.0019]. These estimations are very close to our priliminary estimations using the one week data which we have reported in Jeddi, *et al* 2006, and Figure 3.10. That is 3 out of 1832, which gives point estimation of 0.0016 which is close to the overall estimation of 0.0021.

3.6.2 Theoretical Method

In this method the fitted probability distributions of *LTI* and *ROT* are utilized. It can provide an estimate of the overall performance of the stable system assuming the number of samples is large enough.

We presented estimated distributions for *LTI*, in Table 3.5, and *ROT* earlier in this chapter. Figure 3.11 shows these distributions under IMC for 3 nm pairs. The overlap of these probability distributions suggests that P{*LTI*<*ROT*} is not zero. We note that in fitting the PDF for *LTI*, we have not considered samples of *LTI* for which we could not obtain their corresponding *ROT*. Let $g(\cdot)$ represent PDF of *ROT*, and $F_{LTI}(\cdot)$ represent the Cumulative Density Function (CDF) of *LTI*. Then,

$$p\{LTI < ROT\} = \int_{-\infty}^{\infty} p\{LTI < ROT \mid ROT = x\} \cdot g_{ROT}(x)dx$$
$$= \int p\{LTI < x\} \cdot g_{ROT}(x)dx \qquad (3.4)$$
$$= \int F_{LTI}(x) \cdot g_{ROT}(x)dx.$$

Equation (3.4) cannot be evaluated analytically for the distributions we have chosen. One can estimate (3.4) using stochastic simulation or a numerical method. The result is 0.007, as a point estimation for the pairs of interest in peak-IMC period. Assuming the Poisson process for SRO, a 95% C.I. can be calculated.

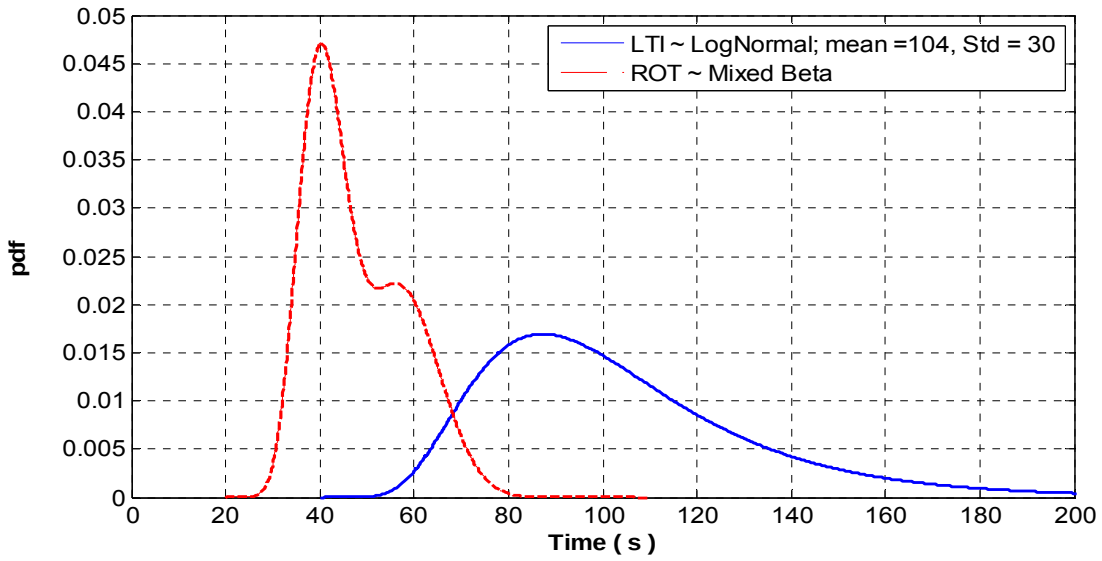

Figure 3.11. Probability distributions of *ROT* and *LTI3* and their overlap

We see that the theoretical estimation 0.007 is about 2.5 times of the empirical estimation 0.0021 for peak-IMC periods. We note that these estimates are optimistic because we have missed about 3.5% of total landings based on the ASPM, and second we could not obtain *ROT* for some peak-IMC landings. These two effects may have added to

P{*LTI*<*ROT*}. That is, they may have had bigger *LTI* than *ROT* of their leading aircraft.

3.7 Chapter Conclusion

We presented an efficient way to use multilateration surveillance system data taking into account and analyzing noise, errors, and missing data. We obtained the wake vortex weight class of 98.6% of aircraft landing in peak periods. We added this information to the multilateration data along with the meteorological conditions that we obtained from the ASPM database. We suggested an algorithm to extract samples of random variables *LTI*, *IAD*, and *ROT* from the data. The samples were conditioned on IMC and VMC times and peak traffic periods in which there were seven or more landings per quarter hour on a given runway. Also, *LTI* and *IAD* were additionally conditioned based on follower-leader wake vortex weight class and aggregated for ones with a minimum separation standard of 3 nm – namely, pairs S-S, L-S, B757-S, H-S, L-L, B757-L, and H-L --, and 4 nm in Table 1.1.

The data supported our assumption that samples of each random variable were independent. We represented the PDF of *IAT* at FAF, *LTI*, *IAD*, and *ROT* by a few known density functions and compared their performance. Fitting distributions to the collected samples showed that *ROT* is best represented by a mix beta distribution, but not with a normal distribution, which is generally assumed in the literature. *LTI* and *IAD* of the follow-lead pairs under study were best fit by log-logistic distributions; however, the log-normal distribution was also accepted for *LTI* and it is easier to work with its variance needed in chapter 4. We also showed that the *LTI* between the leading and following

aircraft is independent of *ROT* of the leading one when *LTI* is under 200 seconds. Our overall observations suggested that there was almost no difference of *ROT* between IMC and VMC conditions, for the observed landings at DTW. We estimated the probability (or frequency) of *LTI*<*ROT* in peak periods with empirical and theoretical methods.

CHAPTER 4 STATISTICAL SEPARATION STANDARDS

In the context of high demand for runways and their scarcity, this chapter is concerned with the problem of how the landing system (in terms of the separation planning and control) should operate. Current separation standards provide minima for any given follow-lead aircraft type as demonstrated in Table 1.1 for instrument flight rule. We discussed some shortcomings of the current separation standards in section 1.3. We explained that an effective separation design shall address two challenges. First it shall control the risk of severe wake vortex encounter, i.e., WV hazard, and simultaneous runway occupancy (or go-around) under peak operations. Secondly it should possibly reduce inherent variability of the separation spacing, which may result in increasing the throughput without increasing the risk. One of the hypotheses in this dissertation is that the current separation design does not posses these characteristics. In this section we propose a framework to set a different type of separation standard to compensate for the weaknesses of the current standards.

This chapter attempts to provide an answer to the second and, partially, to the third questions put forth in Chapter 1. They are: what parameters should a separation standard include to function as an operational guideline and to directly account for variability in the process, and how should the optimal levels of separation standard parameters be

decided to maximize the system output? In this chapter, we first describe a process control oriented approach to analyze the landing phase. Then we formulate a mathematical separation model, and introduce a statistical approach to design a landing separation standard. A numerical example is provided.

4.1 The Final Approach Process

To analyze the behavior of a system it is necessary to obtain an overall view about its operational structure. A process oriented approach provides such a view and this paper models air traffic control operations from this perspective. The following notations are used throughout the chapter.

4.1.1 Notation

- k, k+1 indices of lead and its follow aircraft, respectively
- $LTI_{k,k+1}$ landing time interval between aircraft k and k+1 measured at the runway threshold
- $IAD_{k,k+1}$ inter arrival distance of aircraft k and k+1 when aircraft k is over the threshold
- ROT_k runway occupancy time of aircraft k
- MS minimum separation
- LCL lower control limit
- S_j separation distance between an aircraft pair controlled by controller j
- Δ_j constant buffer added to MS by controller j
- TV_j target value of controller j which is $MS+\Delta_j$

- TV_t time-based spacing target value
- TV_n nmi-based spacing target value
- p_j proportion of aircraft pairs guided by controller *j*
- ε_j separation error from TV_j of controller *j* assumed to have $N(0, \sigma^2_j)$ distribution
- σ_j standard deviation of the imposed control by controller *j*
- α_R acceptable probability for $LTI_{k,k+1}<ROT_k$
- α_{WV} acceptable probability for moderate or severe wake vortex encounter
- μ_{LTI} mean of *LTI* probability distribution
- τ_{LTI} mode of *LTI* probability distribution which is TV_t

The indices are dropped whenever the general parameter or variable is the subject. A variable with a '*' is an optimal value.

4.2 Air Traffic Control Processes

We consider the air traffic control system as a process with inputs and outputs (Figure 4.1). System outputs include throughput, risk, safety, delays, etc. These are the result of various inputs to the system. We cluster the inputs in three categories:

- Operational human participants: pilots, air traffic controllers, and other people involved in the operational decision making process.
- Mid-term plans: standards such as separation standards, procedures such as landing/departure procedures, rules, training curriculum of pilots and air traffic

controllers, decision support systems such as statistical analysis tools designed to give feedback to managers, etc. This cluster of inputs may be revised or changed by high level decision makers in medium terms, for example 3 years.

- Uncontrollable or long-run controllable factors: these are factors for which decision makers have no control in the short-run or have no control at all. They include weather, supply and demand interactions in the market, or long-run changes in aircraft technology, airports, navigation systems, number of runways, etc.

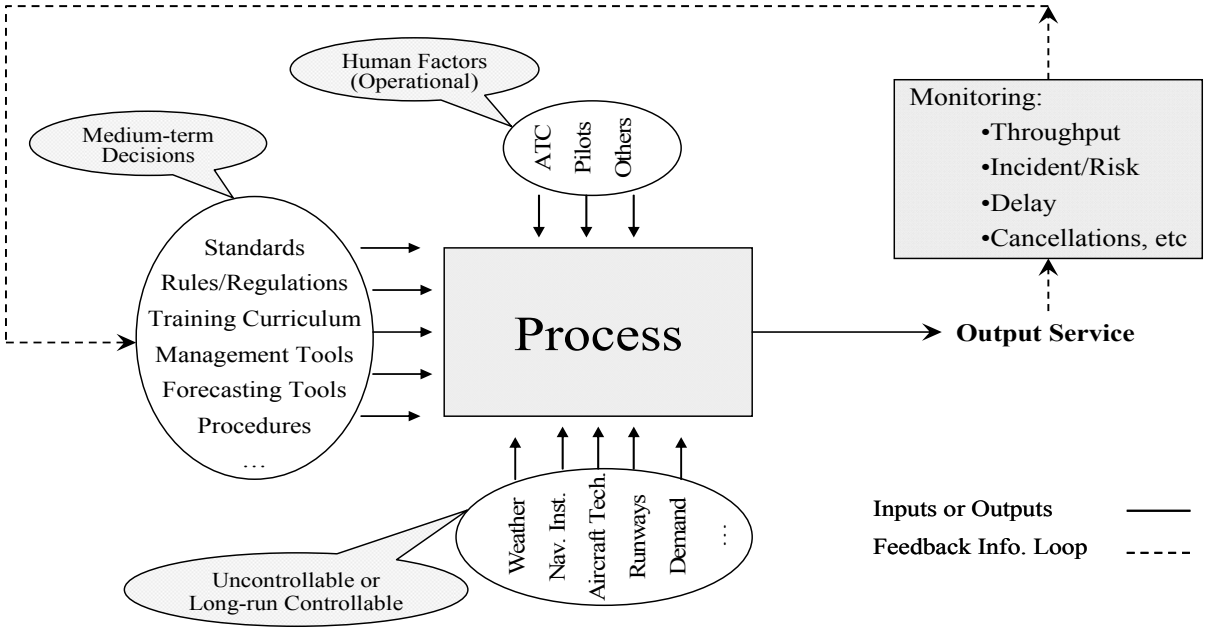

Figure 4.1. Feedback loop on an air transportation process

Output characteristics of the process such as throughput, runway utilization, frequency of incidents, and frequency/length of delays are random variables because of

uncertainty involved in the first and third (and sometimes in the second) categories of inputs. Attempts should be made in probabilistic operations to reduce the variance as much as possible. However, there is always some inherent and uncontrollable variation in the process, which can not be completely eliminated.

4.2.1 Statistical Process Control of the Aircraft Approach Process

Concepts of variability and control are widely developed and employed in the manufacturing industry (Montgomery 2001, and Bowker and Lieberman 1972, for example). In the context of the quality of manufactured items, the natural inherent variability is often referred to as a *stable system* (or *pattern) of chance causes*, and is viewed as an acceptable source of variation. However, any variation in excess of this natural pattern is unacceptable and its detection and possible correction is required. Variations outside the stable pattern are known as *assignable causes* of quality variation. A process which operates in the absence of any assignable causes of erratic fluctuations is said to be *in statistical control*.

We employ the general knowledge of statistics and adopt statistical tools used to monitor stochastic processes in manufacturing, named *statistical process control*, to the approach/landing process. This research introduces a methodology for planning, analyzing, and controlling operations of the approach process, first, to ensure that separation standards will not be violated as a result of high landing demand, and secondly, to reduce output variability to possibly gain a throughput increase.

We assume that the system *capacity* is fixed for a given weather condition and runway and airport infrastructure. Therefore, the *utilization* of a given system/capacity can be improved, but not the capacity itself. We use the term *throughput* to represent the realized number of planes landing per unit of time.

4.2.2 Landing Risks in the Final Approach and Runway

For a given infrastructure (quantity and quality of physical equipment and airport facilities), aircraft capabilities, and weather conditions, the main limiting factor of throughput is the separation spacing between aircraft in the approach phase. This research addresses time and distance separation in the approach phase for a single runway or parallel independent runways.

Separation of an aircraft pair is a random variable due to the nature of the process inputs and components. Figure 4.2 shows final approach path (glide slope). Final Approach Fix is 5.9 nm from the threshold.

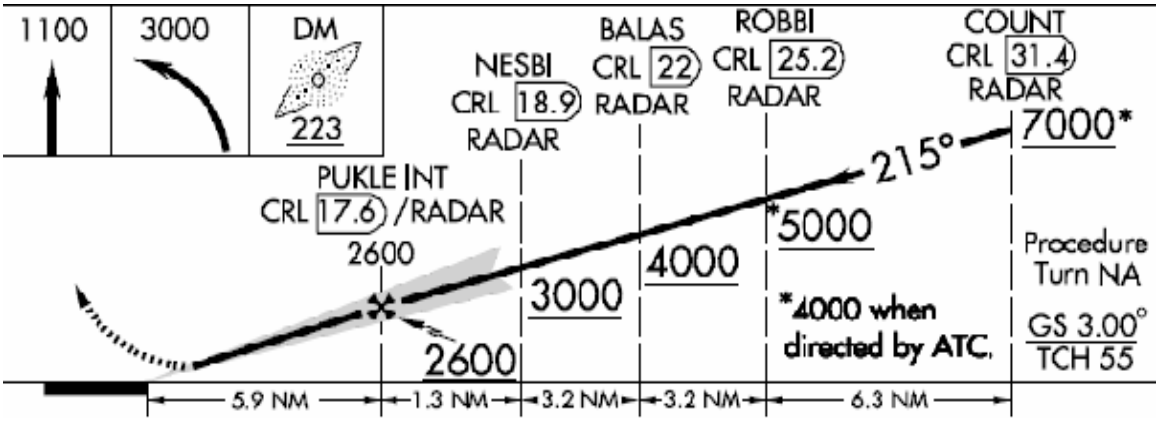

Figure 4.2. A typical final approach process

We categorize pairs of aircraft into four classes of 3, 4, 5, and 6 nm based on the separation standard of Table 1.1 (FAA 1993). (One exception, which is considered for some runways, is a separation standard of 2.5 nm for the follow-lead pairs of small-small, large-small, and large-large aircraft.) The *LTI* probability distribution functions (PDF's) for the individual classes may be different, so we consider them separately in analyzing separation standards. The realized PDF of *LTI* for *all* aircraft is the mixture of the individual class-PDF's, where the class-PDF's are weighted by the fraction of landings under each separation class.

The separation spacing is necessary for two reasons. First, the spacing should be large enough to avoid a simultaneous runway occupancy or runway incursion. Second, the spacing should be large enough to diminish the risk associated with the wake vortex of the leading aircraft.

Under IFR, the air traffic controller (ATC) is responsible to guide aircraft/pilots to assure the separation minima. It is assumed that if these minima are strictly respected, no aircraft cross the threshold to land while the lead aircraft is still on the runway. Thus, it is assumed that $P\{LTI<ROT\}=0$ where *LTI* is measured at the runway threshold.

ROT depends on factors such as the number and structure of exit-ways, touchdown speed, wind velocity along the runway, and aircraft breaking capability. These factors can not be changed easily. So we assume a given PDF for *ROT* and study the possible changes in the PDF of *LTI* and *IAD*.

In peak periods, there is a high landing demand for runways. In such cases, ATC and pilots push aircraft as close as possible to each other to satisfy the arrival demand. This increases the probability of violating the separation minima.

4.3 Statistical Separation Standards

An effective separation design shall address two challenges. First it shall control the risk of severe wake vortex encounter and simultaneous runway occupancy (or go-around) under peak operations. Secondly it shall possibly reduce inherent variability of the separation spacing which may result in increasing the throughput without increasing the risk.

Conceptually, this study models the separation as a random variable and analyzes the nature of its variance. Then we propose an algorithm to set separation standards based on statistical tools which posses' two aforementioned characteristics.

4.3.1 A Mathematical Model for the Separation

Under IFR the ATC is to maximize landing throughput subject to the spacing minima from Table 1.1, for different pair types of aircraft. Index controllers by j=1,…,m. To respect a given *minimum separation* (*MS*), the controller j needs to add a *buffer spacing* Δ_j to the *MS* while pushing as close as possible to the *MS* in order to maximize the throughput. This concept is also suggested by Vandevenne (1992). Adding the buffer Δ_j means that the controller targets a separation value of $TV_j=MS+\Delta_j$, as illustrated in Figure 4.3. In this figure, the leading aircraft is at point 0 and the following aircraft is somewhere on the *IAD* axis. We name the buffered-spacing as *target separation value* or

for simplicity *target value TV*. In this dissertation, we assume that ATC *j* decides on his/her TV_j independently based on his/her experience, cognitive tendency, and level of risk aversion. Thus, TV_j may differ between air traffic controllers.

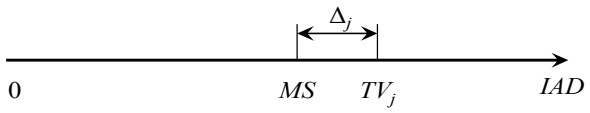

Figure 4.3. A buffer spacing added by ATC *j* to the minimum separation

Assume that a pool of infinitely many pairs of aircraft of a given type, e.g., large-large, is lined up to land on a single runway which is guided by *m* controllers. A pair of aircraft from this pool which is controlled by ATC *j* has a separation S_j which is a random variable. Then

$$S_j = MS + \Delta_j + \varepsilon_j \quad \text{for } j = 1,...,m \tag{4.1}$$

where ε_j represents the random separation error of ATC *j* around his/her target separation. We assume $N(0, \sigma_j^2)$ distribution for the error terms ε_j.

Let p_j be the proportion of the aircraft from this pool which is controlled by ATC *j*. The overall separation *S* of the pool is a mix of separations S_j with proportions p_j, j=1,…,*m*. We can write

$$S = TV + \varepsilon = MS + \Delta + \varepsilon \tag{4.2}$$

where

$$\begin{aligned} &\Delta = \Delta_j \quad w.p. \quad p_j \text{ for } j = 1,..., m \\ &\varepsilon = \varepsilon_j \quad w.p. \quad p_j \text{ for } j = 1,..., m \\ &\textstyle\sum_{j=1}^{m} p_j = 1. \end{aligned} \tag{4.3}$$

Assuming $\varepsilon_j \sim N(0, \sigma_j^2)$ results in a normal distribution for the separations S_j and S in equations (4.1) and (4.2). A normal distribution is also independently suggested by Vandevenne and Lippert (1992), and Xie (2004 and 2005). Haest and Goverts (1995) address the contribution of radar plot accuracy to horizontal separation standards with the normality assumption for displayed polar coordinates on the radar screen.

From (4.2) and (4.3), the expected value of S is:

$$\begin{aligned} E(S) &= E(MS) + E(\Delta) + E(\varepsilon) \\ &= MS + \textstyle\sum_j p_j \Delta_j + \sum_j p_j E(\varepsilon_j) \\ &= MS + \textstyle\sum_j p_j \Delta_j, \end{aligned} \tag{4.4}$$

since MS and Δ_j are constants, and $E(\varepsilon_j)=0$. Also, because $E(\varepsilon_j^2)=\sigma_j^2$, the variance of S is

$$\begin{aligned} Var(S) &= Var(MS) + Var(\Delta + \varepsilon) \\ &= Var(\Delta) + Var(\varepsilon) + 2Cov(\Delta, \varepsilon) \\ &= Var(\Delta) + \left[E(\varepsilon^2) - E^2(\varepsilon)\right] \\ &\qquad + 2\left[E(\Delta \cdot \varepsilon) - E(\Delta)E(\varepsilon)\right] \\ &= Var(\Delta) + \textstyle\sum_j p_j \sigma_j^2, \end{aligned} \tag{4.5}$$

where $Var(MS)$ is zero and the last equality follows by conditioning on j and using $E(\varepsilon_j)=0$. Now, if we fix $\Delta_j=\Delta$ – equivalently, if we fix $TV_j = TV$ (that is, if each controller

uses the same target spacing) – the variation caused by the variable Δ is eliminated. Thus, Var(Δ) is zero, and a new separation S' is obtained with a smaller variance

$$Var(S') = \sum_j p_j \sigma_j^2 \,. \tag{4.6}$$

As a result, it is expected that the *target-value based separation standard* provides a smaller overall variability for any given landing aircraft pair. For the case of two ATC, (4.5) can be written as

$$Var(S) = p_1(1-p_1)(\Delta_1 - \Delta_2)^2 + p_1\sigma_1^2 + (1-p_1)\sigma_2^2 \,. \tag{4.7}$$

By making $\Delta_1=\Delta_2$, the separation variance decreases by the following proportion:

$$\frac{p_1(1-p_1)(\Delta_1 - \Delta_2)^2}{p_1(1-p_1)(\Delta_1 - \Delta_2)^2 + p_1\sigma_1^2 + (1-p_1)\sigma_2^2} \,.$$

The following numerical example illustrates these concepts.

4.3.2 Example

Suppose that two groups of ATC guide landings on a runway under IFR with proportions $p_1=p_2=0.5$ and with equal error variances $\sigma_1^2= \sigma_2^2= \sigma^2$. Table 4.1 shows the variance reduction percentage for the assumed scenarios. The first column is the assumed overall variance of aircraft separation, $Var(S) = 0.45^2$, which is assumed fixed for all scenarios. The second column $|\Delta_1-\Delta_2|$ is the assumed absolute difference between buffer spacing of the two ATC groups. The third column $Var(S')$ is the overall variance of aircraft separation *if the buffer spacings were made equal*: $\Delta_1=\Delta_2$. The last column is the percent

reduction in variance. For example, in the third scenario, changing the difference in buffer spacing from $|\Delta_1-\Delta_2|=0.4$ to $|\Delta_1-\Delta_2|=0$ results in a 20% reduction in the variance of aircraft separation. The values for $\mathrm{Var}(S')$ in the third column were computed by substituting $Var(S') = p_1\sigma_1^2 + p_2\sigma_2^2$ from (4.6) into (4.7), giving:

$$Var(S') = Var(S) - p(1-p)(\Delta_1 - \Delta_2)^2 . \tag{4.8}$$

In this analysis, we do not include separation effects due to gaps in the schedule or the arrival process since the effect of the controller influence is the subject of the study. In particular, equation (4.2) assumes that the aircraft are lined up to land one after another, so we consider no term in the equation representing a possible gap waiting for the next plane to arrive at the terminal airspace. In practice, the aircraft may not be readily present in the line, so some longer separations would be realized that cannot be explained by the normal distribution. So, skewness in the right hand side of the *IAD* (and *LTI*) PDF is expected.

Table 4.1. Variance-reduction scenarios

Var(*S*)	**$\lvert\Delta_1-\Delta_2\rvert$**	$\mathrm{Var}(S')$	**% Var. reduction**
0.45^2	0.2	0.44^2	5
0.45^2	0.3	0.42^2	11
0.45^2	0.4	0.40^2	20
0.45^2	0.5	0.37^2	31

In summary, by introducing a *unified target separation* among all ATC, the variance in the approach phase can be proactively controlled. This may allow the possibility of

having a closer separation spacing (by setting a smaller *TV* or smaller buffer Δ) and higher throughput with a maintained level of risk.

However, the other important side of the story is to provide controllers with a short-run feedback mechanism from the operation. For this purpose, we provide air traffic controllers with complementary values besides target value standards. Specifically, we also provide a Lower Control Limit (*LCL*) for separation spacing and a corresponding probability γ, where it is desired that the proportion of paired landings with separation less than *LCL* is less than γ – that is, $P\{IAD<LCL\}<=\gamma$. Different values of *LCL* can be specified for different probabilities γ. So, *LCL* can be thought of as a function of γ, that is, $LCL(\gamma)$.

4.4 Methodology to Set a Target Value and Lower Control Limit

To set suitable values for the aforementioned separation parameters, i.e. *TV* and *LCL* (for a given probability), we need to observe the long-run system operations to get an insight about the steady state and dominant PDF of *IAD, LTI*, and the imposed control by ATC and pilots; call these long-run PDFs *process characteristics*.

Samples from the probability distribution of the imposed separation are not directly observable (Figure 4.4). A question is how to obtain this PDF using samples of other observable variables such as inter arrival time (IAT) to the terminal radar approach control (TRACON) area and *LTI* to the runway threshold. Xie *et al*. (2004 and 2005) suggest that this transformation function can be modeled as an M/N/1 queue, where the

IAT is exponentially distributed and the imposed spacing distribution is approximately a normal distribution. They estimate the imposed normal distribution around the mode of the *LTI* PDF for the pool of all landings in both peak and non-peak periods. They do not separate peak and non-peak period operations.

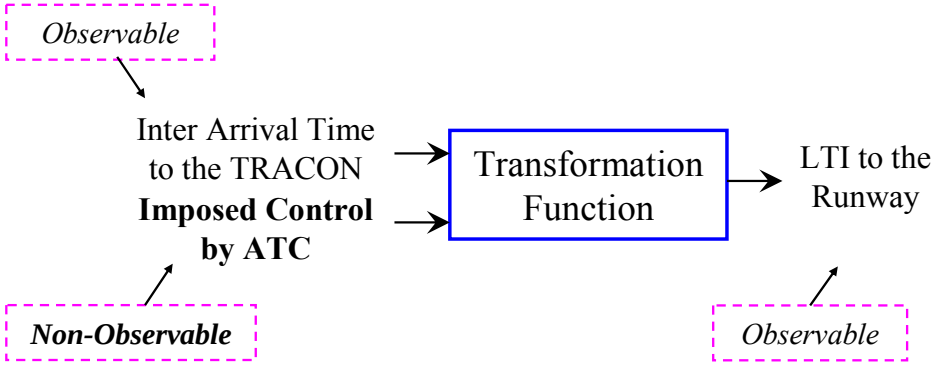

Figure 4.4.Observable and non-observable distributions

We suggest that a more effective approach to address this problem is to find the distribution of *LTI* and *IAD* in peak periods. In this way, the main parts of the larger gaps (which are the result of large arrival gaps to the TRACON area) are systematically eliminated. Then the mode of this distribution represents approximately the mean (or the target value) of the imposed separation, which we assume is normally distributed as discussed earlier. We also assume that the standard deviation of the imposed separation can be estimated from the spread of the observed PDF – for example, by subtracting the observed mode and an observed low-probability quintile. The explicit formula for estimation of the standard deviation is given later in the algorithm, step 5.

Maintaining secure separations is not very challenging in a non-peak period. Problems generally occur in congested traffic times when there is a tendency to land as many aircrafts as possible, and as a result, to reduce the separation. Therefore, we need to obtain the stable pattern of the system behavior, i.e. PDF of *IAD* (and *LTI*), in peak periods. In this research, we assume that periods of seven or more arrivals per quarter hour represent a peak period.

The target value should be set with respect to the following constraints

$$P\{LTI<ROT\} <= \alpha_R, \tag{4.9}$$

and

$$P\{\text{at least moderate wake vortex encounter}\}<= \alpha_{WV}, \tag{4.10}$$

where α_R and α_{WV} are very small values, e.g. 10^{-4}, representing acceptable runway and wake vortex related risk probabilities, respectively.

This dissertation does not address how to set the values for α_R and α_{WV} , but rather assumes the values are given. Also, this dissertation does not address calculation of the probability in (4.10). This could be accomplished through a variety of wake models such as the NASA AVOSS model (Robins *et al*. 2002) or the P2P model (Holzäpfel 2003). Here, we focus on computing the probability in (4.9).

Now, the goal of setting the target value *TV* is to shift the PDF of the landing time interval *LTI* so that the probability in (4.9) is satisfied (in this chapter, we ignore the wake

vortex requirement (4.10)). As we have assumed, the target value *TV* is also the mode τ of the distribution of *LTI*. More specifically, *LTI* shall be shifted so that the average throughput is maximized subject to an upper limit of α_R in (4.9). If different values of the mode τ correspond to shifting the distribution of *LTI* up or down, then the problem can be stated as

$$\begin{aligned} &\text{maximize } E(\text{Throughput}) = \frac{1}{\mu_{LTI}} = \frac{1}{\tau + c} \\ &\text{subject to } P\{LTI(\tau) < ROT\} \le \alpha_R \\ &\qquad\qquad \tau > 0. \end{aligned} \tag{4.11}$$

where *c* is a positive constant equals to $\mu_{LTI} - \tau$.

P{*LTI*(*τ*)<*ROT*}, which is directly proportional to the overlap of *LTI* and *ROT*, gets larger as $TV_t = \tau$ decreases, i.e. P{*LTI*(*τ*)<*ROT*} is monotonically decreasing in *τ* (see Figure 4.5). That is, a bigger overlap of *LTI* and *ROT* implies a bigger P{*LTI*(*τ*)<*ROT*}. Point zero in this figure is the moment that the leading aircraft crosses runway threshold. On the other hand, the average throughput is maximized for the lowest possible *τ*. Thus to solve this optimization model, it is enough to solve (4.9) in its equality form

$$g(\tau) = P\{LTI(\tau) < ROT\} - \alpha_R = 0. \tag{4.12}$$

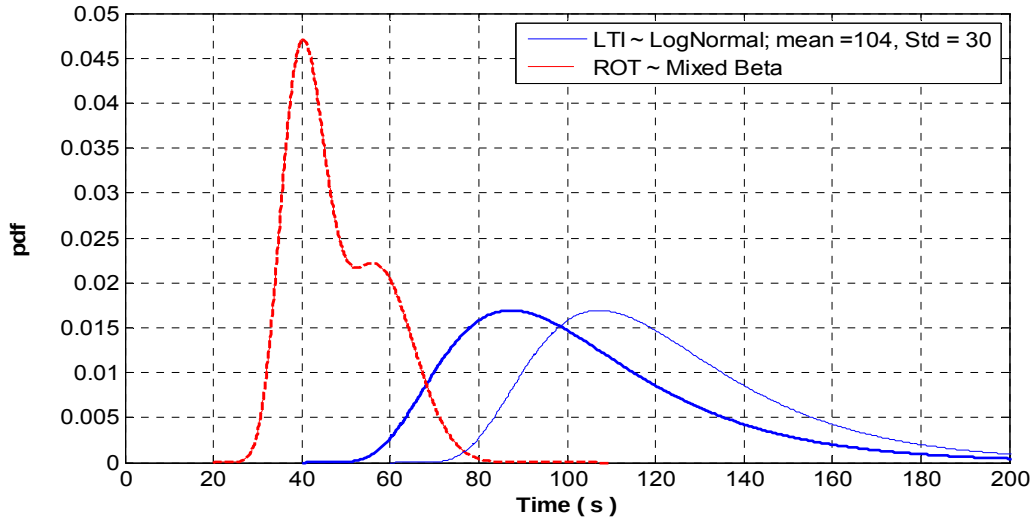

Figure 4.5. Effect of Target Value on the overlap size of *LTI* and *ROT*

We solve this equation for τ using the bisection search method since g(τ) is monotone in τ. P{$LTI(\tau)<ROT$} should be calculated in every step of the bisection search algorithm for a given value of τ using stochastic simulation, for example.

The following algorithm completes and summarizes the discussion of setting the target separation spacing for a given pair of follow-lead aircraft in order to maximize throughput given an upper limit for P{$LTI<ROT$}.

4.4.1 Algorithm

1. Decide on the arrival rate to represent peak landing periods. The mode of *LTI* PDF in these periods can represent the targeted value of the imposed separation in Figure 4.5. Collect a sufficient number of samples from the stable pattern of the process in peak periods over a long period of time during a given weather condition, e.g., instrument meteorological condition (IMC) in this paper.

2. Fit PDF's for *IAD* and *LTI* for different pairs of follow-lead aircraft. For example, we used a Log-Logistic and log-Normal distribution fits in chapter 3. Obtain modes of these distributions in addition to other parameters. Also, fit a PDF for *ROT*. For example, we used a beta distribution fit in chapter 3.
3. Based on outputs from step 2, and by using the bisection algorithm, solve (4.12) for τ for a given upper bound α_R for P{*LTI*<*ROT*}. This provides the time-based target value separation $TV_t^* = \tau^*$.
4. Estimate the average ground speed on the glide slope (the final path ending on the runway which has 3 degree slope in average as illustrated in Figure 4.2) by dividing the mode of the *IAD* PDF by the mode of the *LTI* PDF calculated in step 3. Multiply τ^* by the average speed to obtain the optimum nm-based target value TV_n* separation.
5. Estimate the standard deviation σ of the overall imposed control by the group of ATC, which is assumed normally distributed. Knowing that $P(N(\mu,\sigma^2)<3\sigma) = 0.0013$, estimate σ by $\hat{\sigma} = \left(\text{mode}(LTI) - F^{-1}[0.0013]\right)/3$ where *F* is the CDF of *LTI*. If the target values of ATC's were unified, this standard deviation would estimate the *stable system of chance-causes* deviations from the target value. Apply this step to *IAD* as well. In the long run, after completing the learning curve for the unified target-value separation, the standard deviation shall be considered as part of the separation standard so that any significant divergence from it shall be recognized.

4.4.2 A Monitoring Mechanism

A monitoring mechanism is necessary to assure the process operates as it is designed and the risk is under control. One way is to count the number of times that *LTI* (or *IAD*) is below a certain threshold. If the fraction of observations below the threshold is too large, we conclude the process is out of control. For example, if $F(\cdot)$ is the CDF of the observed process, then it is expected that $100\gamma\%$ of observations lie below $F^{-1}(\gamma)$. For $\gamma = 0.02$, if more than 2% of IMC-peak period *LTI* falls under $F^{-1}(0.02)$, then we conclude that the runway related risk of $P\{LTI<ROT\}$ is out of control, and possible actions shall be taken to find any assignable causes, and make corrections as possible. This might be because the ATC targets smaller separation value, or because the variability has become larger or because of other assignable causes. A monitoring mechanism based on the 2-percentile allows judgment about the process in about 50 landings. On the other hand, if the monitoring mechanism is based on observing a simultaneous runway occupancy – which is a rarer event – it takes many more observations before a judgment can be made.

4.4.3 Numerical Example

Earlier in Chapter 3 (also Jeddi *et al*. 2006), we studied the approach process at Detroit metropolitan Wayne county airport (DTW) using one week of multilateration track data. They provide PDF's for *IAD*, *LTI*, and *ROT* under IMC after showing that samples from each one of these random variables are approximately independent. Then, assuming that these samples are from identical distributions, the "independent identically distributed" (i.i.d.) assumption, which is necessary for distribution-fitting purposes, is satisfied. They also demonstrate that based on their samples ROT_k and $LTI_{k,k+1}$ are approximately

independent. To have sufficient data for the fitting purpose they aggregate the observations for all pairs of follow-lead aircraft that are subject to class-3 nm separation standard. In this section, we use these previous results to illustrate setting up statistically driven target values *TV* for in-trail threshold separation spacing.

4.4.4 Algorithm Illustration

1. We use an arrival rate threshold of seven or more per quarter-hour to represent peak periods. Assume that the four month observation given in Table 3.2 is long enough to represent the steady state system behavior. These are also assumed in Chapter 3 distribution fittings. In Chapter 3, Table 3.5, we obtained 752 samples of *IAD* and 770 samples of *LTI* under IMC for the pairs subject to 3 nm (or 2.5 nm in special cases) minimum separation standard in Table 1.1.
2. According to our analysis in Chapter 3, LogNormal(40; 4.06, 0.45) is a reasonable PDF fit for *LTI* where 40 s is the minimum of *LTI* range, 4.06 is the scale parameter and 0.45 is the shape parameter (see Figure 3.7). The estimated distribution is *ROT*~ 0.59 Beta([20,90],11.8, 27.9) + 0.41 Beta([30,110],9.0,16.6). See Figure 4.5 for PDFs of *LTI3* and *ROT* of small and large aircraft.
3. For this example, let α_R=0.001 and obtain the corresponding mode and shift of the *LTI* PDF to satisfy equation (12) using the bisection search algorithm and stochastic simulation. The expected value of the current P{*LTI*(τ_0)<*ROT*} is calculated as 0.007, for τ_0=87 (or equivalently μ_0=104 for *LTI*) where 0 index indicates the current value. This is more than the desired level of 10^{-3}. Using the

bisection algorithm, the optimal TV_t^* is calculated to be 97 s – that is, the PDF of *LTI* should be shifted by 10 seconds to the right.

4. From the information obtained in Chapter 3, the average in-trail speed is 132 knots (=3600*3.2/87). Then the corresponding shift of *IAD* PDF is 0.3 nm to guarantee P{*LTI*<*ROT*} in 10^{-3} level, in the expected value sense, based on the samples in hand. In this case, nm-based target value TV_n^* of separation for pairs of class-3nm shall be set to 3.5 nm.
5. F_{LTI} is the CDF of Log-Normal(40; 4.06, 0.45). Estimate the standard deviation of the normal control by

$$\hat{\sigma} = \left(\text{mode}(LTI) - F_{LTI}^{-1}[0.0013]\right)/3 = (87 - 40 - 15)/3 = 10.7 \text{ s.}$$

In the same manner, standard deviation of nm-based imposed separation is 0.45 nm. Thus, we may consider the imposed control as $N(3.2,0.45^2)$ (Figure 4.6). From (4.2), this result concludes that the imposed nm-based separation $S=MS+\Delta+\varepsilon$ follows a $N(3.2,0.45^2)$ distribution. In other words, if MS=3.0 nmi, then $E(\Delta)$ is 0.2 nm and $Var(\Delta+\varepsilon)$ is 0.45^2 nm^2. (Note that this is the amount of the variance that we considered for the variance reduction example earlier in this chapter.) In the same manner, the left side of the *LTI* PDF is estimated by $N(87,11^2)$ around the mode 87 s (Figure 4.7). Again, in the terminology of equation (4.2), the time-based separation $S \sim N(87,11^2)$, i.e. $E(MS+\Delta)$= 87 s and $Var(\Delta+\varepsilon)= 11^2$ s^2.

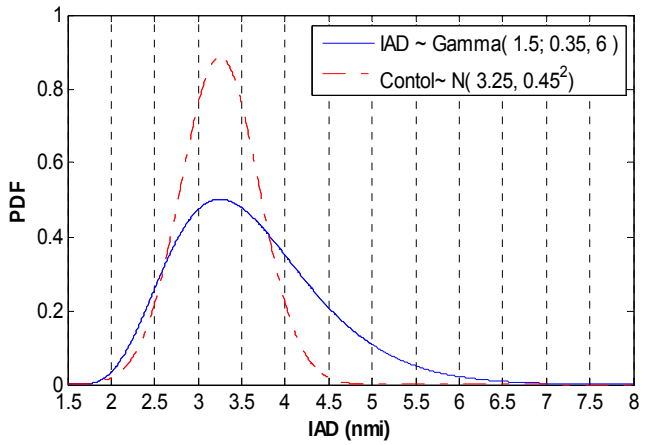

Figure 4.6. IMC-Peak Period *IAD* and the Imposed Control; Feb 2-8, 2003

4.4.5 Monitoring Mechanism Illustration

F_{LTI} is the CDF of log-normal(40;4.04,0.45). $F^{-1}_{LTI}(0.02) \approx 63$ s. If among 100 IMC-peak period landings more than 2% of *LTI* occur under 63 s, conclude that the process does not operate as expected. Causes of such phenomenon shall be identified and appropriate changes in the process shall be applied.

The current average throughput in IMC-peak periods is 8.7 arrivals per quarter-hour, which corresponds to a mean of 104 s for *LTI*. This provides runway related risk of 0.007 in peak-IMC periods. By the shift of +10 seconds, this risk is limited to 0.001, and the average throughput is 7.9 arrivals per quarter-hour.

4.5 Effect of Reducing Separation Variance on the Risk

We would like to know the effect of reducing separation variance on the risk P{*LTI*<*ROT*}. Figure 4.7 shows that the overlap of *LTI* and *ROT* reduces sharply by reducing the variance of *LTI3* while maintaining the mean at 104 s. Accordingly, P{SRO}

reduces from 0.007 to 0.0014 and 0.0002 when we reduce *LTI* Standard Deviation by 30% and 50% from its original value, respectively.

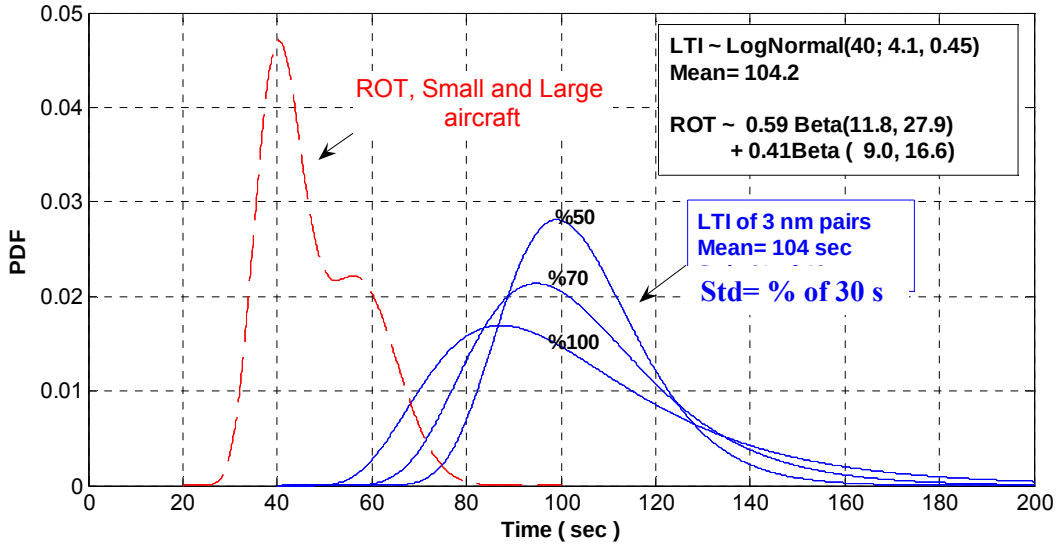

Figure 4.7. Effect of reduced separation variance (or Std) on the overlap of *ROT* and *LTI;* P{SRO} = 0.007, 0.0014 and 0.0002 for the 0%, 30% and 50% reduced Std, respectively

Figure 4.8a shows the relationship between average throughput and the runway related risk (for Feb 2-8, 2003 data). Figure 4.8b represents the relation between safety (defined here to be 1 minus the runway related risk) and the average throughput for the obtained probability distributions of *LTI* and *ROT* (for the one week Feb 2003 data). The risk is increasingly sacrificed as throughput grows. In other words, the second derivative of the risk (safety) in terms of the throughput is positive (negative). For example, raising the average throughput from 8.5 to 9 increases the risk by 0.006 (=0.01-0.004); however for the same amount of increase from 9.0 to 9.5, the risk increases by 0.015 (=0.025-0.01),

which is 2.5 times 0.006. This demonstrates that the rate of the risk increase in throughput is more than linear.

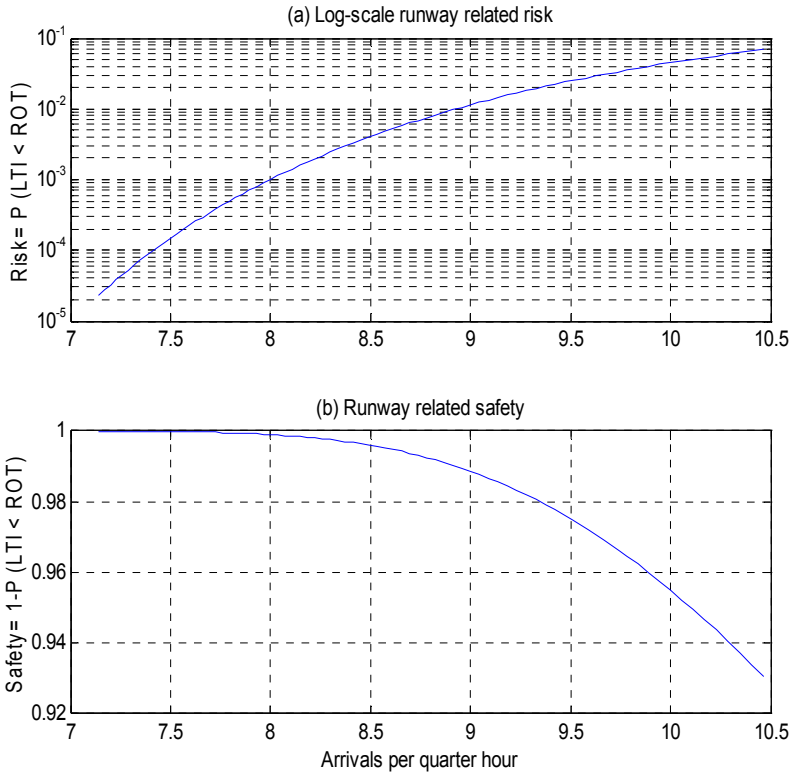

Figure 4.8. Risk and safety as functions of average throughput, Feb 2-8, 2003

Fixing the buffer spacing among all ATC may decrease the variance of *LTI* . In such a case, the buffer spacing can be reduced without increasing the risk of *LTI*<*ROT*. Figure 4.9 shows P{*LTI*<*ROT*} as a function of reduction in *LTI* variance for a fixed amount of 8.5 arrivals per quarter-hour. The figure is drawn on a logarithmic scale.

P{*LTI*<*ROT*} is calculated for *LTI*~ Gamma(40;11·*e*,6/*e*), where *e* is a multiplier in [0.6,1.2]. The variance of the new distribution (after applying *TV*-based standards) is *e*

times the original variance 27^2. From Figure 4.9, if the variance decreases to about 68% of the current value, runway related risk is reduced to 10^{-3} without changing the mean of *LTI* and/or average throughput.

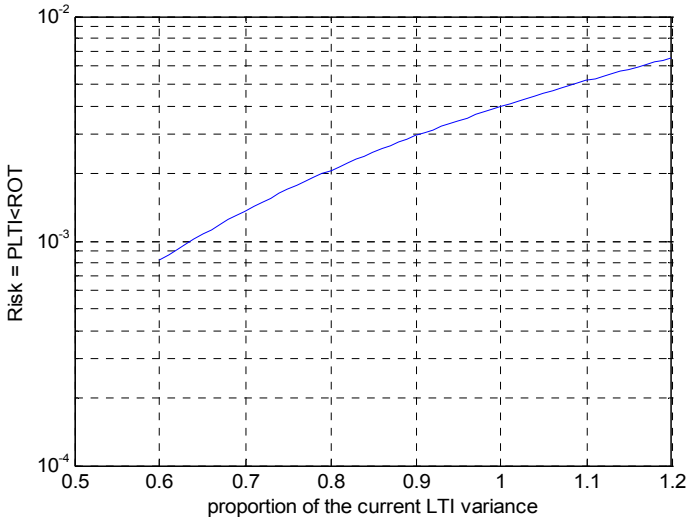

Figure 4.9. P{*LTI*<*ROT*} as a function of reduction in *LTI* variance, Feb 2-8, 2003

In a similar manner, reducing *LTI* variance will decrease the risk of wake vortex hazard.

4.6 Chapter Conclusion

In a process control approach, we modeled the influence of air traffic controllers on the aircraft separation as a random variable with a normal noise. The separation due to gaps in the schedule or arrival process is not the subject of this study and therefore is not included. We verified the observed variance in the current imposed control a result of two factors: 1) the natural inherent variability which we refer to as the stable pattern of chance causes, and 2) the variance outside the stable pattern of the chance causes referred to as assignable causes. The proposed separation model recognizes a systemic assignable

cause in the current separation design. That is, for a given minimum separation standard, controllers add a buffer spacing and target a higher spacing than the allowed minimum separation standard in order to control the chance of simultaneous runway occupancy risk. The buffer spacing may differ among the controllers. We showed in (5) that this difference contributes to the overall variability of *IAD* (and *LTI*), and unifying buffer spacing (and target value) among controllers reduces the overall variance. We showed that if random separation errors of controllers have identical probability distributions, the variance reduction allows a closer spacing (in average) and higher throughput (and capacity utilization) with a maintained level of the risk.

In general, it is not possible to directly sample the imposed control of the arrival process. Therefore, this chapter provided a statistical procedure to estimate the probability distribution of the imposed control given the PDF of *IAD* and *LTI* in peak periods. In this procedure, the mode of *IAD* estimates the average target value of all controllers. $\hat{\sigma} = \left(\text{mode}\left(IAD\right) - F^{-1}\left[0.0013\right]\right)/3$ estimates the standard deviation of the overall imposed nm-based control where F is the CDF of *IAD*. We proposed a new approach to set separation standards using the statistical observations, so the term *statistical separation standards*. The new standard specifies not only a lower bound for the separation but also a standard for the *target value* and the *variance* of the process.

The standard target separation *TV* is calculated by shifting the PDF of *LTI* so that throughput is maximized and P{*LTI*<*ROT*} is remained under a very small given value. The standard variance is of the stable pattern of chance causes, which is calculated after

target separation values are unified for all controllers and the learning curve is completed for the unified target value. We proposed a mechanism to monitor if the spacing process operates as desired over time. Results of Chapter 3 are used to illustrate the methodology, the monitoring mechanism, the possible variance reduction, and the increase of system utilization for a given level of the risk.

This chapter focused on in-trail separation spacing under IFR considering only the runway related risk. However, the proposed model, methodology and procedures are readily adaptable for 1) en-route controlled separations, and 2) accounting for a very limited wake encounter risk. Obtaining further samples from the process is worthwhile for a better estimation of PDF of *IAD*, *LTI*, and *ROT*. A more sophisticated monitoring mechanism of the separation process is necessary to explicitly provide in-action or medium-term feedbacks on the imposed target value and the process variance. However, exploring these problems are not the subjects of this dissertation.

CHAPTER 5 MAXIMIZING THE SYSTEM OUTPUT

In this chapter we analyze the optimal level of operations on a single runway used only for arrivals. The statistical estimations of chapter 3 are used in optimization models. The chapter mainly answers the third problem, i.e., what is the optimal level of the target separation as the main component of the in-trail statistical separation standard introduced in Chapter 4.

5.1 Background

As discussed in chapters 1 and 2, there is increasingly high demand for runway slots (landing or departure) during peak periods at congested airports. The expense of runways and the high demand have made them very limiting and economically valuable resources of the air transportation network. The limitation of runway and airport capacity is a major cause of delays in the network. Thus, it is desirable to obtain the maximum possible output of the runway operations. The objective of this chapter is to understand the probabilistic dynamics of landing operations and to estimate runway capacity based on these dynamics while also considering go-around procedures to mitigate risk.

There are extensive studies regarding capacity estimations and throughput maximizations of airports, see Gilbo (1993), for example. Railsback *et al*. (2005)

provides an overview of methods and tools used to estimate runway capacities. Our study is focused on landing/approach operations only. Early studies of landing capacity go back to the 1940's when runways became congested and delays became a concern. Capacity is commonly considered a constant rate as the reciprocal of the minimum-allowed / safe-time spacing between aircraft – e.g., Bowen *et al*. (1948), and Bell (1949). In a classical capacity study, Blumstein (1959) focused on landings under instrument flight rules (IFR) when an aircraft separation is required prior to the final approach and the velocity differences cause loss of capacity. In a more recent study, Lang *et al*. (2003) study the possibility of increasing throughput by using cross-wind information in sequencing the landings on closely spaced parallel runways. Some other works and tools are used to evaluate the capacity and delay benefits of different operating scenarios, for example Boesel (2004).

This chapter is concerned with optimization of landing operations on a single runway for a given pair of follow-lead aircraft, large-large for example. In this dissertation, two major safety risks in aircraft landing procedures are considered. These are the risks of a wake vortex (WV) hazard and the risk of simultaneous runway occupancy (SRO). A wake-vortex hazard occurs when the following aircraft enters the wake vortex of its leading aircraft. When the wake is strong enough, the encounter may cause a loss of control, which may result in passenger injuries or even fatalities. SRO risk is the probability that a following aircraft reaches the runway threshold before the leading aircraft exits the runway. SRO is a precursor for a physical collision on the runway.

These risks are to be avoided to assure a safe landing. Separation requirements to mitigate these risks are the major constraints on the capacity of the runway.

Existing probabilistic approaches to this problem study the relation between these risks (or safety) and throughput rate; see for example Xie *et al*. (2003 and 2005), Levy *et al*. (2004). The maximum throughput occurs at the point of maximum allowable risk. For example, in Chapter 4 we illustrated a methodology for the case of a restricted SRO probability. We considered the probabilistic nature of aircraft separation and set the maximum throughput so that the probability of a SRO equals some pre-specified small value. However, the SRO risk was not completely eliminated from the operations. In this chapter, we eliminate these risk factors from the operations by considering "go-around" (GA) or "missed approach" procedures, Nolan (2003). We assume that such procedures are strictly enforced and respected whenever the separation distance is below a specified threshold. The optimal level of operations is determined to maximize the number of successful landings, while also considering (and minimizing) the number of arriving aircraft that must take a go-around. Numerical examples here are based on probability distributions of landing time interval (*LTI*) and runway occupancy time (*ROT*) for Detroit Metropolitan airport estimated in Chapter 3 (Jeddi *et al*. 2006). These distributions are for the pairs with 3 nmi FAA minimum separation standard (FAA 1993).

In the next sections we first explain *GA enforced* or *risk-free* landing operations. We formulate a model to maximize landing throughput and to find the optimal level of

operations to maximize the economic output. A mathematical model is presented to optimize the output given a fleet mix.

5.1.1 Notation

The following notations are used throughout the paper. The input parameters are:

- $LTI_{k,k+1}$ landing time interval between aircraft k and k+1 measured at the runway threshold in seconds and assumed to have the lower limit L
- ROT_k runway occupancy time of aircraft k measured in seconds
- B dollar benefit of one successful landing
- C expected average cost of a go-around or unsuccessful landing
- x_0 minimum wake vortex safe separation of successive aircraft given in seconds
- MAP1 missed approach point 1; nm distance from threshold where pilot/controller decides whether to execute go-around procedure to avoid SRO. This is known as the decision height under precision approach.
- MAP2 missed approach point 2; nm distance from threshold where pilot/controller decides whether to execute go-around procedure to avoid hazardous wake vortex encounter

The decision variables are:

- ω landing attempts per hour, i.e., flow rate through the glide slope, and ω = 3600 / mean(LTI)

- λ arrival rate to TRACON or, equivalently, the runway throughput rate, landing per hour
- *p* probability of go around P{GA}

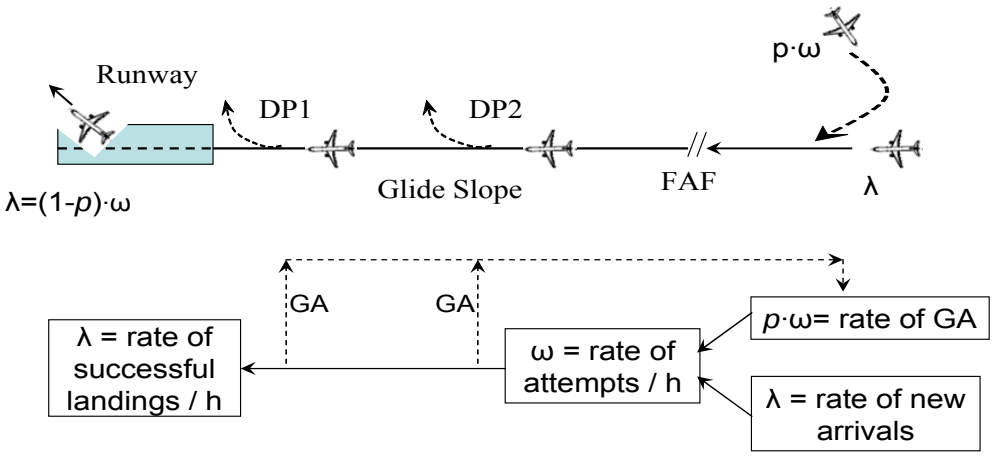

Figure 5.1. Go-around procedures on the glide slope

5.2 Go-around Enforced (Risk-free) Landing

It is desired that the chance of a simultaneous runway occupancy or a WV hazard, i.e., moderate or severe encounter, be nearly or exactly zero. In conventional models in the literature, increasing the target separation between successive aircraft decreases these two risks. The risk can also be reduced by implementing go-around procedures. For example, if two aircraft will be on the runway at the same time, the trailing aircraft can execute a go-around procedure to avoid a SRO. In reality, the go-around is not always taken.

In this chapter, we assume that an aircraft is *always* enforced to execute a go-around whenever separation minima are not or will not be met. This will be discussed later. In addition, we assume complete information to make this decision. With these assumptions,

the risk of a SRO or a wake-vortex hazard is exactly zero, though there is possibly an increase in the number of go-arounds.

Making the system risk-free by enforced GA creates a different dynamic and may change the optimal level of operations, i.e., the best number of attempts per hour. As we show in later sections, the optimal level of attempts per hour depends on the GA probability P{GA} as well as other factors. This section calculates this probability for two cases of with and without wake vortex effect.

In the approach / landing process, two different aircraft flows can be recognized: the flow through the glide slope ω measured in landing *attempts* per hour, and the flow through the runway (or simply throughput) λ measured in *successful landings* per hour. Figure 5.1 demonstrates this dynamic with enforced GA procedures. When the following aircraft is at decision point 2 (MAP2), e.g., 8 nm from runway threshold, the controller/pilot decide(s) whether or not to take a GA procedure to avoid the risk of encountering a hazardous wake from the leading aircraft. We suppose that if the separation is less than a specific value x_0, at MAP2, then the following aircraft must go-around to a holding position and return to the glide slope when cleared to attempt again. Such a minimum WV safe separation exists and can be estimated using wake vortex theories (Xie 2005, Robins 2002, Holzäpfel 2003), for example, and/or field observations, Shortle *et al*. (2006). We name this operation as the "*wake vortex GA*" or "*wake vortex missed approach*" procedure in contrast with the well known GA procedure executed to avoid a SRO. We call the latter a "SRO GA" or "SRO missed approach". In

this paper, for illustration purposes, we consider MAP2 to be 8 nm from the threshold, and x_0 = 55 s separation as the minimum WV safe separation.

If a safe separation is achieved at MAP2, then the aircraft continues the approach. At MAP1, which is well known as missed approach point (or *decision height* under precision approach) the follower decides whether or not to execute a go-around to avoid simultaneous runway occupancy with its leading aircraft (Nolan 2003).

We define p to be the total GA probability that may occur at MAP2 or MAP1. Note that p is a function of the number of attempts per hour ω. The average GA rate (number of go-arounds per hour) is $p(\omega)\cdot\omega$ and the average successful landing rate is

$$\lambda(\omega) = [1-p(\omega)]\cdot\omega. \tag{5.1}$$

The rate of aircraft attempting to land is the arrival rate of aircraft $\lambda(\omega)$ plus the rate of aircraft executing a go-around $p(\omega)\cdot\omega$. As a check for consistency, the attempt rate is $[1-p(\omega)]\cdot\omega + p(\omega)\cdot\omega$ which equals ω, see Figure 5.1.

In addition, we make the following *assumptions*:

- $LTI_{k+1,k}$ and ROT_k are independent random variables
- The separation is minimized at MAP2 and remains unchanged afterwards until the touchdown. In other words, the separation at MAP2 equals *LTI*
- Shifting *LTI* to the right or left does not change the shape of its probability distribution

- Zero risk assumed for execution of both GA procedures
- GA are absolutely respected and enforced at both decision points
- The number of GA in an hour is not restricted
- Wake vortex GA and SRO GA conditions never simultaneously occur for a pair. That is, no simultaneous go around for aircrafts k and k+1 happens for all k=1,2,….

Where $LTI_{k,k+1}$ is the landing time interval between aircraft k and k+1 measured at the runway threshold (in seconds), and ROT_k is the runway occupancy time of aircraft k (measured in seconds).

5.3 Probability of Go-Around Assuming No Wake Vortex Effect

In this section, we ignore the possible go-around at MAP2. In other words, we only consider the risk of a SRO and not the risk of a hazardous wake vortex encounter. The probability of a SRO is

$$\begin{aligned} P\{SRO\} &= P\{LTI < ROT \ \& \text{ Follow aircraft lands}\} \\ &= P\{\text{Follow aircraft lands} \mid LTI < ROT\} * P\{LTI < ROT\}. \end{aligned}$$

This probability can be reduced to zero by enforcing the go around procedure. In this case, P{Follow aircraft lands | $LTI < ROT$}= 0, and

$$p_1(\omega) = \mathrm{P}\{\mathrm{GA}\} = \mathrm{P}\{LTI < ROT\}. \tag{5.2}$$

We estimated probability distribution functions of peak period *LTI* and *ROT* for DTW in Chapter 3 for the pairs of FAA 3 nm minimum separation. These follow-lead aircraft pairs include S-S, L-S, B757-S, H-S, L-L, B757-L, and H-L indicated in FAA (1993). The estimations are used here for methodology illustrations. *LTI* is the peak period distribution calculated for arrival of aircraft to the glide slope (or the final approach fix) with the rate ω.

Figure 3.11 illustrated the *LTI3* and *ROT* probability distributions obtained in Chapter 3 for 3 nm pairs. $p(\omega)$ is estimated as 0.007, the mean of *LTI* is 104 s, and the average number of attempts per hour (during peak periods) is $\omega = 3600/104 = 34.6$ attempts/h. In this period, no go-around was observed, so $\omega = \lambda$, but $P\{SRO\} = 0.007$ instead of 0.0.

We assume that changes in arrival rates (that is, changes in λ or ω) can be modeled by shifting the *LTI* distribution to the left or right, i.e., by changing the location parameter. Shifting the *LTI* distribution also changes the probability that *LTI*<*ROT*, or equivalently, the probability of a go-around. $p(\omega) = P\{LTI < ROT\}$ is given by broken line in Figure 5.2.

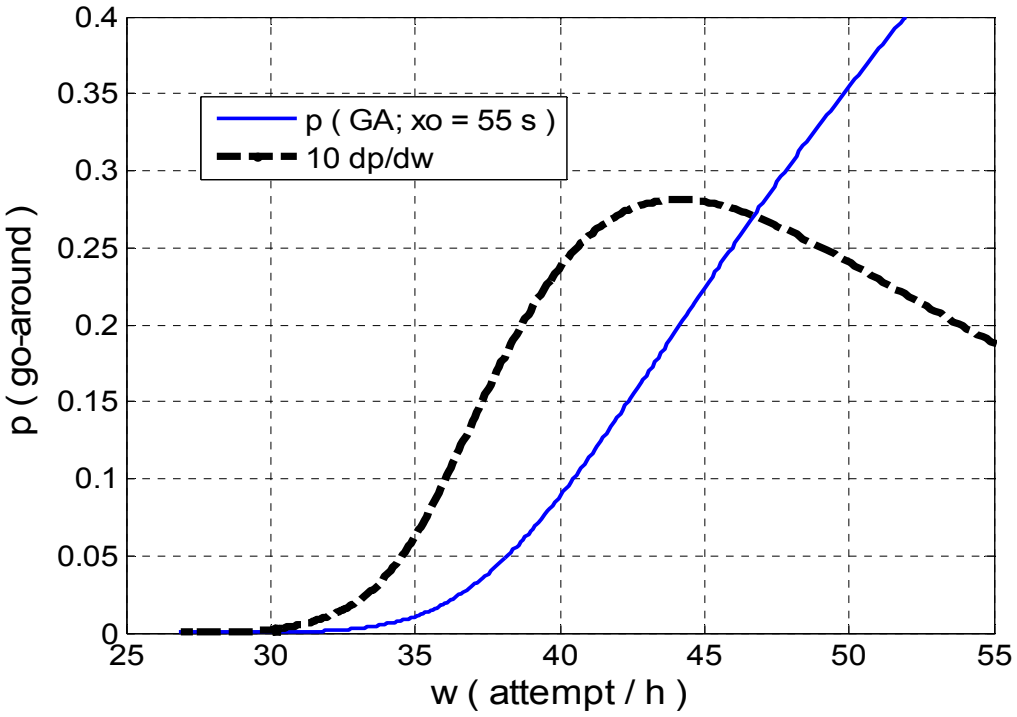

Figure 5.2. Total P{GA} and 10 times of $dp/d\omega$

5.4 Total Probability of Go-Around with Wake Vortex Effect

When the wake vortex effect is taken into account and WV GA procedure is in place, an aircraft would possibly miss the approach for two reasons at two different points: WV safe threshold and runway safe threshold (so-called missed approach point). For this situation, let x_0 to be the minimum wake vortex safe separation of successive aircraft given in seconds, and L to be the lower limit of *LTI* distribution; e.g., L = 40 sec. Figure 5.3 illustrates a wake vortex safe threshold x_0 given PDFs of WV strength in time and *LTI*3.

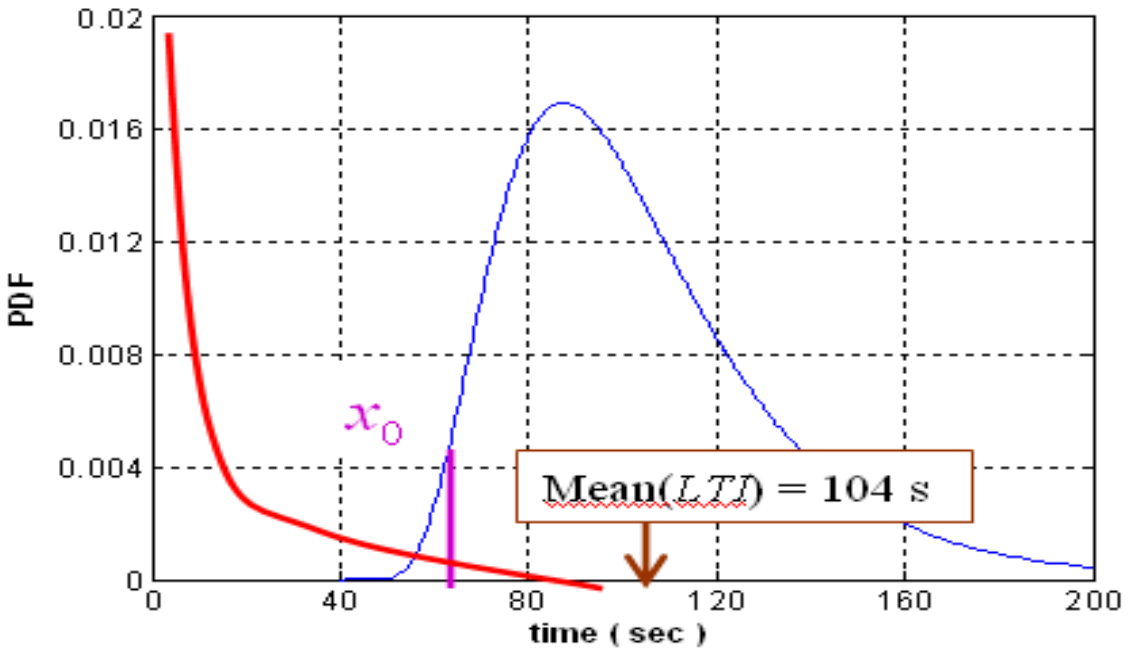

Figure 5.3. PDFs of WV strength and *LTI* with illustrated WV safe threshold x_0

We estimated and discussed *LTI* distribution in Chapter 3. This *LTI* is a representative of the process capability. In the current situation (based on the collected samples) no severe wake vortex encounter has been reported. To estimate the safe wake vortex threshold, we use the process capability considering the assumption of no wake vortex encounter. Thus, from Table 3.5, we can see that aircraft can be as close as 48 seconds without no hazards for 3 nm pairs. We add 7 seconds for the reaction time in order to execute go-around procedure to avoid wake vortex hazard, which results in x_0= 55 seconds where P{ *LTI*3 < x_0= 55}= 0.0013. For 4 nmi pairs we decided 75 sec as the safe threshold.

To calculate P{GA} two cases for L and x_0 shall be considered as follows:

Case 1: $L < x_0$. For this case

$$P\{GA\} = \int_{x_0}^{\infty} F_{LTI}(y) dF_{ROT}(y) + F_{LTI}(x_0) F_{ROT}(x_0), \tag{5.3}$$

where F_{LTI} and F_{ROT} are CDF of *LTI* and *ROT*, respectively.

Case 2: $L >= x_0$. This case means that *LTI* shifted to the right as much that its lower point L is above the wake vortex safety threshold of x_0. No wake vortex GA would ever occur in this case, and P{GA} is obtained from equation (5.2).

Total $p(\omega)$ = P{GA} is shown in Figure 5.3 for peak period DTW IMC distributions (see Figure 3.11) and for x_0 = 55 s. Figure 5.3 also shows p_1 and derivative of $p(\omega)$ in terms of ω. The derivative $dp/d\omega$, which will be used in the following sections, is multiplied by 10 to make it more visible in this figure.

Having P{GA} as a function of average rate of landing attempts, in the next sections we formulate some models to analyze the tradeoff between the cost of go-around and throughput given an absolutely safe landing.

5.5 Maximizing the Net Economic Benefit

We are meant to adjust average landing attempt rate ω to maximize the overall output of the landing system, while P{SRO}= P{WV hazard}= 0 is maintained by enforced GA procedure. Optimal ω will introduce the GA rate $p(\omega)$. On the other hand, since this is an economic system, the overall output may be well represented by the overall net economic benefit to all the system beneficiaries. System beneficiaries include airlines, passengers,

airports, employees, etc. It should be noted that, maximizing the number of (successful) landing rate does not necessarily guarantee the overall economic optimality of the landing operations. This is because the relative quantities of costs and benefits influence the optimality and should be taken into account. However, we will show that maximizing the successful landing rate is a special case of maximizing the overall net economic gain.

For the landing operations when absolute safety is guaranteed by enforced GA procedure, the total net economic gain is the result of a successful landing and the overall cost of a possible go-around procedure. The landing benefit is the total revenue to all beneficiaries minus operational cost, except the cost of GA execution. The net economic benefit, that is, total benefit minus total cost of an hour of peak period operations, is desired to be maximized with respect to the average number of attempts per hour, ω. Since this net benefit is a random variable, we consider maximizing expected value of the net benefit, i.e., *ENB*.

The gain from one successful landing is B which occurs with probability 1-$p(\omega)$ for every landing attempt. The loss of one landing attempt is the cost of go-around C which occurs with probability $p(\omega)$. Thus, since the number of attempts per hour is ω, then the expected value of the net gain from hourly landing attempts is $ENB(\omega;B,C)$ given in (4) and the optimization objective is

$$\text{Maximize } ENB(\omega;B,C)=\omega\cdot\left[(1-p(\omega))\cdot B-p(\omega)\cdot C\right]. \tag{5.4}$$

For any given type of aircraft, C is the summation of cost components such as passenger delay cost, disturbed schedules cost of downstream flights, take off cost, aircraft operations cost, and airport cost. Any of these cost components depend on parameters such as aircraft load factors and the arrival rate at a given time, which are uncertain. Thus, C is a random variable. However, we consider its expected value as a suitable estimation of this parameter. Estimation of B and C is not a subject of this paper, but their effect on the optimal level of operation is modeled. However, we will illustrate the concepts and models for some assumed quantities of C and B.

To obtain a more general model, we write *ENB* in terms of the ratio *C/B*. Factoring out B in equation (5.3) gives

$$\begin{aligned} ENB(\omega; B, C) &= B \cdot \omega \cdot \left[(1 - p(\omega)) - p(\omega) \cdot \frac{C}{B} \right] \\ &= B \cdot \omega \cdot \left[1 - \left(1 + \frac{C}{B} \right) p(\omega) \right] \cdot \end{aligned}$$

Thus $ENB(\omega;B,C)$ is a multiplication of constant dollar value B and a function of ω. Define the latter function to be $g(\cdot)$ as

$$g(\omega; r) = \omega \cdot [1 - (1 + C/B) p(\omega)].$$

Or, from (5.1),

$$g(\omega; r) = \lambda(\omega) - \frac{C}{B} \cdot \omega \cdot p(\omega).$$

Thus, maximizing $g(\omega;r)$ is equivalent to maximizing $ENB(\omega;R,C)$. So we can write the problem in a more general form

$$\text{Maximize } g(\omega;C/B) = \lambda(\omega) - \frac{C}{B}\cdot\omega\cdot p(\omega). \tag{5.5}$$

The optimal solution $\omega^*(C/B) = \text{Argmax}\{g(\omega;C/B)\}$ depends on the ratio C/B. The derivative of $g(\omega;C/B)$ with respect to ω is zero at ω^*. $ENB(\omega;B,C)$ and $g(\omega;C/B)$ have the following interesting properties (at least for the *LTI* and *ROT* distributions in hand).

5.5.1 Properties of g(ω;*C/B*)

- **Property 5.1:** For a given B and C, $ENB(\omega;B,C)$ and $g(\omega;C/B)$ are unimodal in a practical peak period rates of [28,55] attempt/h. That is, they have a unique maximum in this range. This is the necessary optimality condition. We will demonstrate this fact later in this section; however, it remains to be proven mathematically.
- **Property 5.2**: $g(\omega;C/B)$ decreases as C/B increases for any fixed ω. This follows directly from equation (5.5). The only term that includes C/B is the term inside the brackets which is decreasing in C/B.
- **Property 5.3**: $g(\omega;r) \to \lambda(\omega) = (1 - p(\omega))\cdot\omega$ when $C/B \to 0^+$. This property is obvious from equation (5.5). So, $g(\omega; C/B)$ is bounded by $\lambda(\omega) = [1- p(\omega)]\cdot\omega$ and lies inside of it, see Figure 5.4 and 5.5 for illustration.
- **Property 5.4**: $\omega^*(C/B) = \text{Argmax}\{g(\omega;C/B)\}$ is decreasing in C/B for $28<\omega<\text{Argmax}\{dp/d\omega\}$. This property is proven in the Appendix.

These properties generalize the behavior of the function g(.) and help to understand the nature of interactions among the problem parameters and their influence on the output. They are illustrated later in this section.

5.5.2 Special Case: Maximizing Runway Throughput

From Property 5.3, when *C* is negligible in comparison with *B*, the problem reduces to maximizing runway throughput $\lambda(\omega) = [1- p(\omega)]\cdot\omega$. By increasing the rate of attempts ω, the percentage of GA increases but the percentage of successful landings decreases. So that, after a point the decrease in the rate of successful landings dominates the increase in the rate of attempts. In other words, throughput λ(ω) has a unique maximum or optimal point. This can also be explained in mathematical terms. $p(\omega)>0$ is increasing, and $1- p(\omega)$ is decreasing in ω. So after a point, decrease of $1- p(\omega)$ dominates increase of ω and $[1-p(\omega)]\cdot\omega$ would have a maximum.

We note that the highest throughput value is a good estimation of the average runway *landing capacity*. So, using this methodology the risk free landing capacity of a single runway can be estimated.

5.5.3 Illustration

We now illustrate these concepts using distributions from chapter 3, see Figure 3.11. In section 2, we obtained the rate of GA $p(\omega)$ for two cases of without wake vortex effect, and with WV effect (having the safe WV threshold of x_0=55 sec), see Figure 5.3. *LTI* and *ROT* distributions are assumed for Large-Large aircraft in peak period, with 3 nm separation minima, under IMC. Note that ω = 3600/mean(*LTI*) where *LTI* is in seconds.

Let C = \$4,000 in average for a large aircraft in a peak period, and assume three scenarios of \$1,000, \$2,000, and \$4,000 for B.

5.6 Optimal Solution without Wake-Vortex Effect

First consider the case where WV effect is ignored. In this case, $p(\omega)$ is calculated from equation (5.1) and plugged into the problem (4), or equivalently into the problem (5), to maximize the expected economic benefit. Figure 5.4 illustrates this case for function $g(\omega;C/B)$. One can plot $ENB = B*g$, for any given B. For this plot, C/B is from {4, 2, 1, 0} from the bottom curve to the top one, respectively. These $g(\omega, C/B)$ are unimodal with unique maxima for a given C/B, as Property 5.1 indicates. The ones with larger C/B ratio lie under the other ones, i.e., Property 5.2. The solid curve at the top corresponds to C/B = 0 and represents the throughput $\lambda(\omega)$, i.e., Property 5.3. Also, as in Property 5.4, peak of $g(\omega;C/B)$ moves down and left by increasing the relative amount of GA penalty to the landing benefit, i.e., the maximal ω^* decreases as C/B increases. Argmax$\{dp/d\omega\}$ is calculated 49.7 attempts/h for the *LTI* and *ROT* in hand, needed for Property 5.4.

The optimal (ω,λ,p) is (46.5, 39.6, 0.148). To have a stable landing system, the arrival rate to the TRACON, λ, is adjusted so that ω is maintained in the optimal level of 46.5 attempt/h. At most, 39.6 landings/h can successfully go through the runway; that is, capacity is 39.6 landings/h for this case.

As other examples, for $C=B$, $(\omega, \lambda, p)^*$ = (40.0, 38.2, 0.045). For $C = 2B$, $(\omega, \lambda, p)^*$ = (38, 37.1, 0.024). The latter means that to maximize the expected value of the net economic gain (surplus) from the landing operations, when go-around cost C is 2 times

larger than landing benefit B, the average glide slope throughput shall be adjusted at 38.2 attempts/h which gives 37.0 successful landings/h. For a plot of $ENB(\omega;B,C)$ see Jeddi (2007).

5.7 Optimal Solution with Wake-Vortex Effect

Now, we consider the wake vortex hazard risk in maximization of runway throughput. In this case the problem is maximizing (5) or (4), where $P\{GA\} = p(\omega)$ is calculated from equations (5.3) and (5.2), for x_0= 55 sec. Figure 5.5 illustrates this case for function $g(\omega;C/B)$. One can plot $ENB = B \cdot g$, for any given B, which would give the same optimal solutions. For this plot, C/B is 128, …,2, 1, 0, from the bottom curve to the top one, respectively. All four properties of $g(\omega, C/B)$ can be verified from this plot. It is unimodal, the ones with larger C/B ratio lie under the other ones, the top curve for C/B = 0 represents the throughput $\lambda(\omega)$. and the maximal ω^* decreases as C/B increases. Argmax$\{dp/d\omega\}$ is calculated 41 attempts/h when wake vortex safe threshold is 55 s, see Figure 5.3. This is the condition for property 5.4.

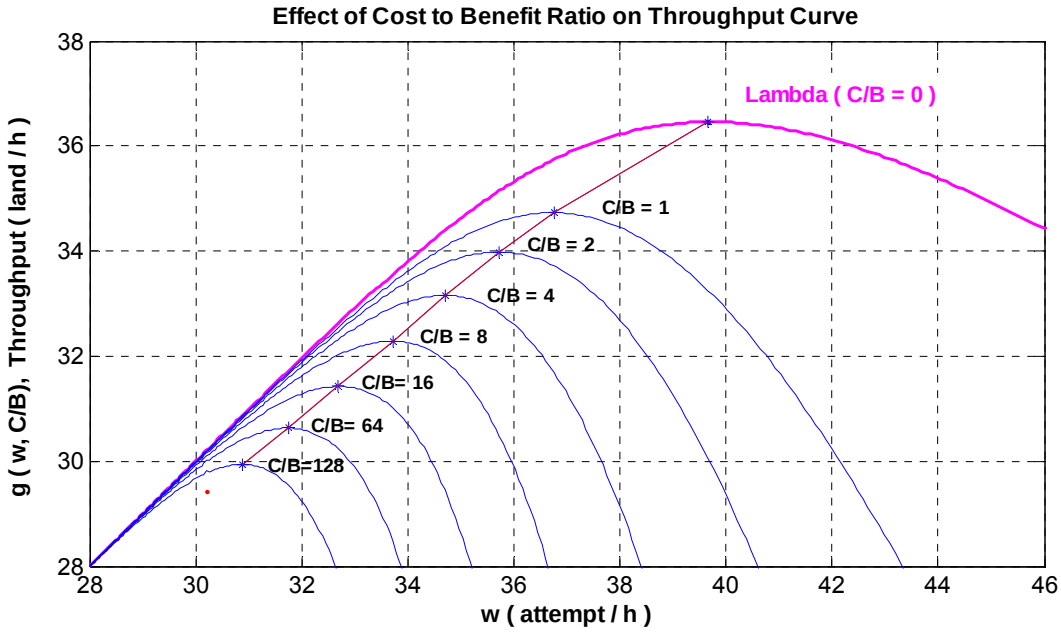

Figure 5.4. g(ω;*C/B*) of 3nm Pairs for *C/B* = 0, 1, 2, …, 128; WV effect included

Optimal values of this figure are summarized in Table 5.1along with optimal values for safe WV thresholds of $x_0 = 55$ and 60 seconds. The optimal solution $(\omega, \lambda, p)^*$ is (39.7, 36.5, 0.081) for $(x_0, C/R) = (55, 0)$. Since $C/B = 0$, that is, cost of go-around is negligible in comparison with the landing benefit, then this is the optimal number of landings/h and the maximum achievable throughput. So the average *landing capacity* of the system is 36.5 landings / h independent of the market condition. $(\omega, \lambda, p)^*$ is (35.7, 35.1, 0.016) for $(x_0, C/B) = (55,2)$, meaning that the optimal throughput is 35.1 landing/h if $C = 2B$ in the market, that is, the cost of go-around is two times bigger than the profit gained from a successful landing. Note that in Table 5.1 optimal throughput decreases as safe WV threshold increases; however, eventually the safe threshold is a certain number and once it is recognized other cases become irrelevant.

Table 5.1. Optimal values for different safe WV thresholds and *C/B*

	WV threshold x_0 = 55 sec			WV threshold x_0 = 60 sec		
C/B	**ω***	**λ***	***P****	**ω***	**λ***	***P****
0	39.7	36.5	0.081	37.8	35.1	0.071
1	36.8	35.7	0.027	35.2	34.5	0.022
2	35.7	35.1	0.016	34.4	34.0	0.013
4	34.7	34.4	0.009	33.6	33.4	0.007

We can now obtain an interesting estimation. WV is costing the system 39.6- 33.5 = 6 landings per peak hour. That means WV cost is about 21,900 landings per year if there is 10 hours of peak periods every day. This is for the cases of 3 nmi pairs, which majority of them are large aircrafts. Now we can multiply this value by *B* and obtain dollar value WV cost estimation. For *B* = \$1000, we have about \$22 m per year for a single landing runway under IMC.

As a closing discussion for this section some capacity estimations would be helpful. As we mentioned in the introduction, the reciprocal of the minimum safe separation is sometimes considered as an estimation of the capacity. Using that method for the safe minimum separation of 65 s, one obtains the capacity of 55.4 landings per hour. We can intuitively recognize that this number is too high since in practice the landing capacity is generally between 30 and 40 landings per hour per runway. The problem with this method is that it ignores the probabilistic nature of the process. Achieving this level of throughput requires that the mean of *LTI* to be adjusted at 65 s which implies P{GA} >= 0.55 from Figure 5.2. In other words, with the enforced go-around procedure, there will be more than 55% loss of attempted landings at either MAP. This would lead to the throughput level of less than 25 landing / h. Further, in such an operation the system

should tolerate the high cost of 16 go-around per hour. So this reciprocal method is not suitable.

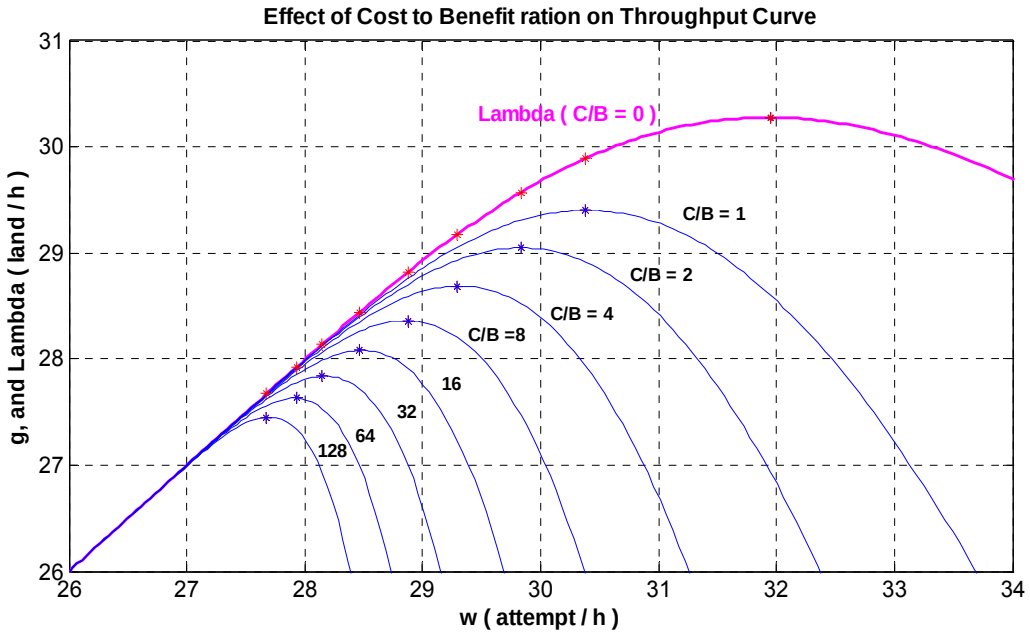

Figure 5.5. g(ω;*C/B*) of 4nmi Pairs For *C/B* = 0, 1, 2, …, 128; WV effect included

Our methodology, which considers the probabilistic behavior of the system, estimated the average capacity of 33.6 landings per hour for 55 s safe WV threshold and risk free landings. Economic considerations may reduce the optimal throughput to about 32 landings / h with a maximized net economic gain, 1% go-around and risk free (safe) operations.

5.8 Optimal Operations for a Given Fleet Mix

In the previous section, we considered the optimal economic operations for a given follow lead aircraft, large-large, for example. In practice, different mix of small, large,

B757, and heavy aircraft land on a runway. This creates a mixture of different follow-lead pairs, for example large-heavy, and each pair may have a different safe WV threshold since the chance of WV hazard depends on the weight class of the leading and following aircraft. In the previous section, thresholds of 65, 70, and 75 s were considered for large-large pairs for illustration.

In this section we extend models (4) and (5) for the case of a varied fleet mix to verify the optimal levels of landing attempts for every given pair in an integrated manner. For a general fleet mix, ω_{ji} attempts per hour results in $P\{GA_{ji}\} = \omega_{ji} p(\omega_{ji})$ for aircraft type j. The total go-around probability for aircraft type j is

$$P\{GA^{j}\} = \sum_{\forall ji} P\{GA_{ji}\}.$$

We assume that the percentage of go-around does not change the fleet-mix of attempting aircraft, that is, α_{ji} remains constant throughout the entire peak period. This assumption is not very limiting firstly, because it is almost valid for small go-around probabilities and, secondly, small percentage of specific fleet mix (like H-S) results in a small rate of go-around (like GA^{H}).

The throughput rate of pairs ji is

$$\lambda_{ji}(\omega_{ji}) = [1 - p(\omega_{ji})] \cdot \omega_{ji},$$

which occurs with α_{ji} proportion. Then the total throughput is

$$\lambda\left(\vec{\omega}\right) = \sum_{\forall ji} \alpha_{ji} \cdot \lambda_{ji}\left(\omega_{ji}\right)$$
$$= \sum_{\forall ji} \alpha_{ji} \cdot \left(1 - p_{ji}\left(\omega_{ji}\right)\right) \cdot \omega_{ji},$$

where $\vec{\omega} = (\omega_{SS}, \omega_{SL}, \ldots, \omega_{HH})$ is the landing attempts for pairs (i,j).

Let B_j be the total benefit of a successful landing (excluding the cost of flight) and C_j be the average go-around cost of aircraft type j. Note that B_j and C_j are the same for aircraft j for all types of its leading aircraft i. Similar to equation (5.4), the expected net benefit from landing operations of pair ji is

$$ENB_{ji}\left(\omega_{ji}; B_j, C_j\right) = B_j \omega_{ji}\left[1 - p_{ji}\left(\omega_{ji}\right)\right] - C_j \omega_{ji} p\left(\omega_{ji}\right)$$
$$= B_j\left[\lambda_{ji}\left(\omega_{ji}\right) - \frac{C_j}{B_j}\omega_{ji} p\left(\omega_{ji}\right)\right].$$

Similar to the single mix case, let

$$g_{ji}\left(\omega_{ji}; C_j / B_j\right) = \lambda_{ji}\left(\omega_{ji}\right) - \frac{C_j}{B_j}\omega_{ji} p\left(\omega_{ji}\right).$$

Then $ENB(\omega_{ji};\ B_j,\ C_j) = B_j \cdot g_{ji}(\omega_{ji};\ B_j,\ C_j)$. Pair ji contributes in total benefit with proportion α_{ji}. Then the total expected net benefit of one hour landing operations is

$$ENB\left(\vec{\omega}; \vec{B}, \vec{C}\right) = \sum_{\forall ji} \alpha_{ji} ENB_{ji}\left(\omega_{ji}; B_j, C_j\right) = \sum_{\forall ji} \alpha_{ji} B_j g_{ji}\left(\omega_{ji}; C_j / B_j\right).$$

Thus, we write the objective as

$$\underset{\vec{\omega}}{\text{Maximize}} \quad ENB\left(\vec{\omega};\vec{B},\vec{C}\right)=\sum_{\forall ji}\alpha_{ji}B_j g_{ji}\left(\omega_{ji};C_j/B_j\right) \tag{5.6}$$

where $\vec{B}=\left(B_S,B_L,B_{B757},B_H\right)$ and $\vec{C}=\left(C_S,C_L,C_{B757},C_H\right)$.

5.8.1 Solution of the Model

Each summation component in equation (5.6), i.e., $\alpha_{ji}B_j g_{ji}(\omega_{ji};B_j,C_j)$, includes only the terms involving *ji*. This means that $ES\left(\vec{\omega};\vec{B},\vec{C}\right)$ is a separable function in *ji*, and its partial derivatives in ω_{ji}, which is needed to obtain the maximal points, does not include other terms. Then to maximize total *ENB* it is sufficient to maximize every ENB_{ji} with respect to ω_{ji} for given B_j and C_j. Or, because $\alpha_{ji}B_j$ are constant values, then it is sufficient to find the solutions of sub-problems

$$\underset{\omega_{ji}}{\text{Maximize}} \quad g_{ji}\left(\omega_{ji};C_j/B_j\right)=\lambda_{ji}\left(\omega_{ij}\right)-\frac{C_j}{B_j}\omega_{ji}\,p\left(\omega_{ji}\right), \tag{5.7}$$

for all *ji*. $\omega_{ji}^{*}=Arg\max\left\{g_{ji}\left(\omega_{ij};C_j/B_j\right)\right\}$ is the solution for problem (5.7). Problems (5.6) and (5.7), for all *ji*, are equivalent.

In Section 5.3 we discussed four properties of function *g*. They are true for $g_{ji}(\omega_{ji};B_j,C_j)$ for all *ji* if $P\{GA_{ji}\}=p(\omega_{ji})$ have similar characteristics, for all *ji*, as $p(\omega)$ in the previous case. In other words, the properties are independent of the type of follow-lead aircraft pair.

5.9 Effect of Reducing Separation Variance on Optimal Throughput

In section 4.5 and Figure 5.7 we discussed and illustrated the effect of reducing separation *LTI* standard deviation (or variance) on P{*LTI*<*ROT*} while maintaining the mean at a constant level 104 s. Here we show the effect of *LTI* variance reduction on optimal throughput. For simplicity, we limit the analysis and examples to the case where C<<B, i.e. *C/B* = 0, without loss of generality. Figure 5.6 shows the effect of reducing standard deviation of *LTI3* and *LTI4* up to %50 of their original values which are 30.4 s and 31.9 s for *LTI*3 and *LTI*4, respectively, while keeping their averages constant. For example, %30 decrease of *LTI*3 Std, leads to 3.6 land/h extra throughput. Other values are seen on the plots.

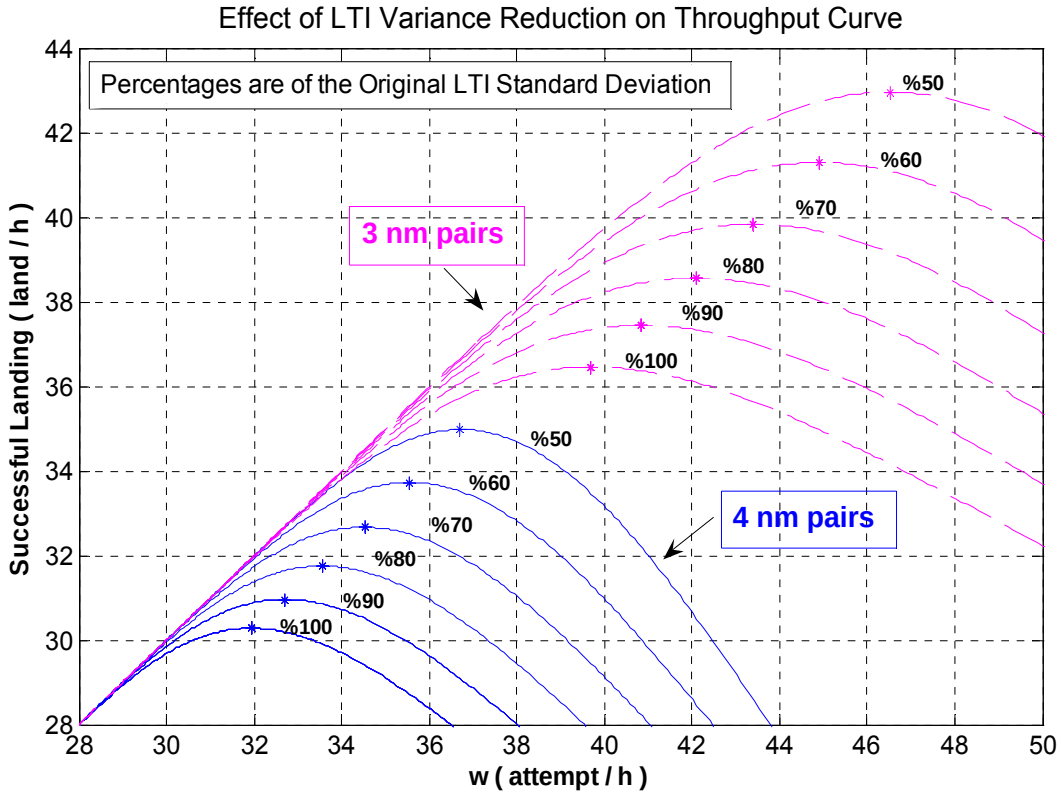

Figure 5.6. Effect of reducing *LTI3* and *LTI4* standard deviations to a percentage of their original values

CHAPTER 6: CONCLUSION

In this dissertation, we studied the landing and approach process to a single independent runway which is solely used for landing operations. The goal is to take the most advantage of runways as a scarce and increasingly demanded resource of the air transportation network. Increasing utilization is achievable by reducing aircraft separation spacing; however, it has trade offs with risking landing safety and human lives. Through this research, we initiated several steps to manage this trade off and to maximize the utilization:

1. We analyzed stochastic properties of the landing process to obtain estimates for the PDF's of inter-arrival distances, landing-time intervals at FAF and runway threshold, and runway occupancy times. From the observed data, the frequency of simultaneous runway occupancy was on the order of 10^{-3}. These results were obtained through processing of multilateration surveillance system data at Detroit airport (DTW).
2. As separation standard parameters, we proposed a statistical separation standard, which includes a *target value* and a *lower control limit* for separation of a given type of aircraft pair. The proposed standard can reduce the variability of the landing separation. Such a standard has the possibility to lead to a quicker realization of safety degradation before observing a major incident. In addition, we demonstrated

how specifying different levels of target separations leads to a trade-off between risk and throughput.

3. These first steps formed the basic building blocks for a model to optimize throughput level without compromising safety, i.e. without increasing the risk. To maintain safety, we proposed a go-around procedure to avoid wake vortex incidents and to assure the landing safety. These go-around (or missed approach) procedures shall be enforced for the sake of safety.
4. Under the enforced go-around procedures, shortening the average separation spacing will increase the go-around rate. We suggested that despite the increased go-around rate, the overall landing throughput rate can still be increased. One optimization model developed to mimic this dynamic of the system. This model is solved for the peak period landing distributions of Detroit airport, and the results supported our hypothesis of increased throughput.
5. The aforementioned optimization model estimates *landing capacity* of the runway, with or, hypothetically, without the presence of wake vortex effect. The maximum achievable safe throughput for 3 nmi pairs, mainly large-large aircraft, is 39.4 per hour when wake vortex effect is ignored. This maximum reduces to 36.5 when 55 sec is considered as the safe wake vortex missed approach threshold. The difference between these estimates provides a logical framework to estimate the economic effect of wake vortex phenomenon in the system. Using these figures we roughly estimated the cost of WV phenomenon (for Detroit airport case assuming two landing runways and 10 hours of peak period per day) as about 10,600 landings of large aircraft per

year. This translates to WV cost of tens of millions of dollars per year in a moderately busy airport.

6. We hypothesized that maximizing the throughput (by adjusting the average separation spacing) does not necessarily assure the most economic use of the runway. Another model developed to mimic these economic dynamics of the approach operations accounting for the go-around cost (to all economic beneficiaries) and the befit of every successful landing (to all economic beneficiaries). System beneficiaries include airlines, passengers, airports, employees, etc. We showed that economically optimal level of operations depends on cost to benefit ratio rather than depending on specific values of go-around cost and successful landing benefit. This validated the hypothesis.
7. We extended the optimization models, which described in conclusions 5 and 6, to obtain the optimize level of landing operations for a given landing fleet mix.
8. We discussed and demonstrated the effect of reducing separation variance on the landing risks, go-around rate, and on the optimal level of landing operations (or throughputs).

We illustrated the methodologies for specific pairs of follow-lead aircraft (using landing distributions of Detroit airport) without loss of generality. Numerical results further validated the methodologies.

APPENDIX A. PROOFS AND DERIVATIONS

Proof of Property 5.4: The proof is by contradiction. $\omega^*(C/B)$ is the point where $dg/d\omega=0$ or $p(\varpi^*)+\varpi^* \cdot p'(\varpi^*)=1/(1+C/B)$. In the alter equation, increasing r decreases the right hand side and consequently the left hand side of the equation. On the other hand, ω, $p(\omega)$, and $dp/d\omega$ are all increasing in ω for $\omega<\text{Argmax}\{dp/d\omega\}$. Thus if ω does not decrease, the left hand side will not decrease. This is a contradiction, and completes the proof.◄

Derivation of equation (5.3): For the case $L < x_0$, note that

$$\begin{aligned} P(GA) &= P\{\text{separation at DP2} < x_0 \text{ or, exclusively, separation at DP1} < ROT\} \\ &= P\{LTI < x_0 \text{ or } LTI < ROT\}. \end{aligned}$$

Then,

$$P(GA) = P(LTI < x_0) + P\{LTI < ROT \text{ and } LTI \geq x_0\}. \tag{A.1}$$

On the other hand,

$$
\begin{aligned}
P\{LTI < ROT \text{ and } LTI \geq x_0\} &= \int_{x_0}^{\infty}\int_{x_0}^{y} dF_{LTI,ROT}(x,y) \\
&= \int_{x_0}^{\infty}\left[\int_{x_0}^{y} dF_{LTI}(x)\right] dF_{ROT}(y) \\
&= \int_{x_0}^{\infty}\left[F_{LTI}(y) - F_{ROT}(x_0)\right] dF_{ROT}(y) \\
&= \int_{x_0}^{\infty} F_{LTI}(y) dF_{ROT}(y) - F_{LTI}(x_0)\cdot\int_{x_0}^{\infty} dF_{ROT}(y) \\
&= \int_{x_0}^{\infty} F_{LTI}(y) dF_{ROT}(y) - F_{LTI}(x_0)\cdot(1 - F_{ROT}(x_0)) \\
&= \int_{x_0}^{\infty} F_{LTI}(y) dF_{ROT}(y) - F_{LTI}(x_0) + F_{LTI}(x_0) F_{ROT}(x_0),
\end{aligned}
\tag{A.2}
$$

where F_{LTI} and F_{ROT} are CDF of *LTI* and *ROT*, respectively. Joint distribution of *LTI* and *ROT*, $F_{LTI,ROT}$, is broken into multiplication of their marginal distributions because of their independence. Using (A.2) in (A.1) gives equation (5.3).

APPENDIX B. INSTRUMENT APPROACH PROCEDURE OF RUNWAY 21L

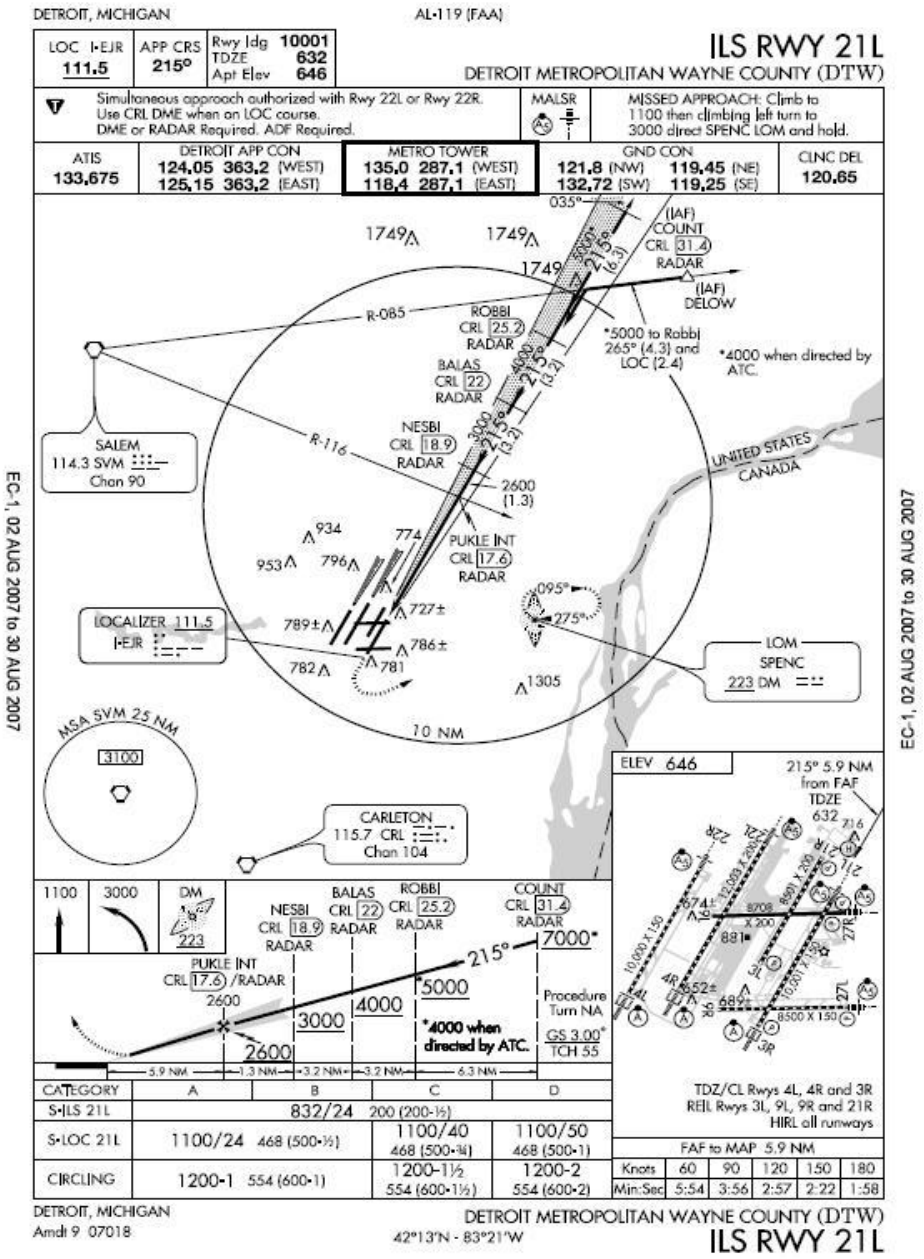

REFERENCES

REFERENCES

1. Andrews, J.W., Robinson, J.E. (2001). Radar-based analysis of the efficiency of runway use. AIAA Guidance, Navigation, and Control Conf., Quebec.

2. Ashford, N, Wright, P.H. (1992). Airport Engineering, 3rd Ed., John Wiley & Sons, Inc.

3. Ballin, M.G., Erzberger, H. (1996). An analysis of landing rates and separations at the Dallas/Fort Worth International Airport. NASA, Tech. Memo. 110397.

4. Bell, G.E. (1949). Operational Research into Air Traffic Control, Journal of Royal Aeronautical Society, Vol. 53, pp 965-976.

5. Blumstein, A. (1959). The Landing Capacity of a Runway. Operations Research, Vol. 7, No. 6., pp 752-763.

6. Boesel, J., Bodoh, D. (2004). Simulating airspace redesign for arrivals to Detroit Wayne county airport. Proceedings of Winter Simulation Conference, pp. 1318-1325.

7. Bowen, E.G., T. Pearcey (1948). Delays in the Flow Air Traffic. Journal of Royal Aeronautical Society, Vol. 52, pp 251-258.

8. Bowker, A.H., Lieberman, G.J. (1972). Engineering Statistics, 2nd Ed, Prentice-Hall, Inc.

9. Donohue, G. (2004). Presentation: Air transportation system is a complex adaptive system, not an air traffic control automation problem. Harvard University.

10. Federal Aviation Administration. DTW Airport Diagram, AL-119, 16 Feb 2006, Available http://204.108.4.16/d-tpp/0602/00119AD.PDF

11. Federal Aviation Administration. (1993). Air Traffic Control. FAA Order 7110.65, Wake Turbulence, Para 2,1,19

12. Federal Aviation Administration. (1993). Same Runway Separation, FAA Order 7110.65, Wake Turbulence, Para 3,9,6

13. GAO (2000). Aviation Safety, Safer Skies Initiatives Has Taken Initial Steps to reduce accident rates by 2007. Report to subcommittee on aviation. Committee on aviation and infrastructure, House of Representatives, United States General Accounting Office.

14. Gilbo, E.P., (1993). Airport Capacity: representation, estimation, optimization, IEEE Transactions on Control Systems Technology, Vol. 1, No. 3, pp. 144-154.

15. Haest, M., Govaerts, B. (June 1995). A Statistical Hypothesis Testing Approach to the Determination of Supportable Aircraft Separation Standards. IEEE AES Systems Magazine.

16. Haynie, C.R. (2002). An investigation of capacity and safety in near-terminal airspace for guiding information technology adoption. Ph.D. dissertation, Dept. Sys. Eng. and Oper. Res., George Mason Univ., Fairfax, VA.

17. Hemm, R., *et al*. (1999). Benefit Estimates of Terminal Area Productivity (TAP) Program Technologies. NASA/CR-1999-208989.

18. Hollander, M, Wolf, D.A. (1999). Nonparametric Statistical Methods, 2nd Ed., John Wiley & Sons, Inc.

19. Holzäpfel, F. (2003). Probabilistic Two-Phase Wake Vortex Decay and Transport Model, Journal of Aircraft, Vol. 40, No. 2.

20. Jeddi, B.G., Shortle, J.F., Sherry, L. (2006). Statistics of the Approach Process at Detroit Metropolitan Wayne County Airport, Presented in 2nd ICRAT conference, Serbia and Montenegro.

21. Jeddi, B.G. (2004). Preliminary Exploration of DROMSIV data on Detroit Airport (DTW). Center for Air Transportation Systems Research, GMU, Internal report.

22. Jeddi, B.G., Shortle, J.F., Sherry, L. (2006). Statistical separation Standards for the Aircraft –Approach Process, Proceedings of 25th Digital Avionics System Conference, Portland, OR, pp. 2A1-1 to 2A1-13.

23. Lang, S., Mundra, A., Cooper, W., Levy, B.S., Lunsford, C.R., Smith, A.P., Tittsworth, J.A. (2003). A Phased Approach to Increase Airport Capacity Through Safe Reduction of Existing Wake Turbulence Constraints, Air Traffic Control Quarterly, Vol. 11, No. 4, pp. 331-356.

24. Law, A.M. (2000). ExpertFit: user's guide, Averill M. Law & Associates

25. Lee *et al*., (1997, April). Estimating the effects of the Terminal Area Productivity Program. NASA Contractor Report 201682.

26. Lebron, J.E. (1987). Estimates of Potential Increases in Airport Capacity Through ATC System Improvements in the Airport and Terminal Areas. MITRE Corporation, Report no. FAA-DL5-87-1.

27. Levy, B., Som, P., Greenhaw, R. (2003). Analysis of Flight technical Error on Straight, Final Approach Segments, 59th Annual Meeting Proceeding of Institute of Navigation, Albuquerque, New Mexico.

28. Levy, B., Legge, J., Romano, M., (2004) Opportunities for improvements in simple models for estimating runway capacity. presented at the 23rd Digital Avionics Systems Conference, Salt Lake City, UT.

29. Montgomery, D.C. (2001). Introduction to Statistical Quality Control, 4th Ed, John Wiley & Sons Inc.

30. Nolan, M.S. (2003), Fundamentals of Air Traffic Control, 4th Ed., Brooks/Cole Publishing Company.

31. Railsback, P., Sherry, L. (2006). A Survey of Rationales and Methods for Determining Declared Airport Capacity. Presented at Annual Meeting of the Transportation Research Board

32. Rakas, J., Yin, H. (2005). Statistical modeling and analysis of landing time intervals: case study of Los Angeles International Airport, California. Transportation Research Record: Journal of the Transportation Research Board, No. 1915, 2005, pp. 69-78.

33. Robins, R.E., Delisi, D.P. (2002). NWRA AVOSS wake vortex Prediction Algorithm Version 3.1.1, NASDA/CR-2002-211746.

34. Rodrigue, J.P., Comtois, C., Slack, B. (2006). The Geography of Transportation System. Routledge.

35. Sherry, L., *et al*. (1999). Closing the Controller/Pilot Loop in the CNS/ATM TRACON: FMS Features to Support CTAS in the TRACON, Honeywell publication C69-5370-011.

36. Shortle, J.F., Jeddi, B.G. (2007). Probabilistic Analysis of Wake Vortex Hazards for Landing Aircraft Using Multilateration Data. Presented at 86th Transportation Research Board Annual Meeting, Washington DC.

37. Vandevenne, H.F, Lippert, M.A. (2000). Using maximum likelihood estimation to determine statistical model parameters for landing time separations. 92PM-AATT-006.

38. Xie, Y., Shortle, J, Donohue, G. (2003) Runway landing safety analysis: a case of Atlanta Hartsfield airport," presented at the 2003 Digital Avionics Systems Conf., Indianapolis, IN.

39. Xie, Y., Shortle, J., Choroba, P. (2004). Landing safety analyses of an independent arrival runway, presented at the 2004 Int. Conf. for Res. in Air Trans., Zillina, Slovakia.

40. Xie, Y. (2005). Quantitative analysis of airport runway capacity and arrival safety using stochastic methods. Ph.D. dissertation, Dept. of Sys. Eng. and Oper. Res., George Mason Univ., Fairfax, VA.

CURRICULUM VITAE

Babak Ghalebsaz Jeddi received his BS degree in Industrial Engineering (IE) in 1994. While in undergraduate program, he co-founded and established the first technical journal of Industrial Engineering and Operations Research (OR) in Iran, which has been managed and operated by students. After obtaining his degree in IE, he worked as a Project Control expert, Strategic Planning expert and Strategic Planning Supervisor while continuing his graduate studies. In addition to IE and OR, his academic studies include courses in Master of Business Administration. He has done consulting in the areas of quality and productivity engineering, including ISO 2000 quality standards. His research interests are in uncertainty, probabilistic and optimization modeling of service and manufacturing systems. He considers economic aspects as critical part of his pragmatic research. His papers and innovative ideas have been awarded in international conferences.